BEHAVIOUR OF HIGH-STRENGTH CONCRETE COLUMNS UNDER ECCENTRIC COMPRESSION - TIED COLUMNS

A THESIS SUBMITTED TO
THE GRADUATE SCHOOL OF NATURAL AND APPLIED SCIENCES
OF
THE MIDDLE EAST TECHNICAL UNIVERSITY

BY

ERDEM CANBAY

IN PARTIAL FULFILLMENT OF THE REQUIREMENTS FOR THE DEGREE

OF MASTER OF SCIENCE

IN

THE DEPARTMENT OF CIVIL ENGINEERING

MIDDLE EAST TECHNICAL UNIVERSITY

ANKARA

AUGUST 1995

Approval of the Graduate School of Natural and Applied Sciences

Prof. Dr. İsmail TOSUN

Director

I certify that this thesis satisfies all the requirements as a thesis for the degree of Master of Science.

Prof. Dr. Doğan ALTINBİLEK

Chairman of the Department

This is to certify that we have read this thesis and that in our opinion it is fully adequate, in scope and quality, as a thesis for the degree of Master of Science.

Assoc. Prof. Dr. Güney ÖZCEBE

Supervisor

Examining Committee Members

Prof. Dr. Ergin ATIMTAY

Prof. Dr. Uğur ERSOY

Prof. Dr. Tuğrul TANKUT

Prof. Ş. Muvaffak ÜZÜMERİ

Assoc. Prof. Dr. Güney ÖZCEBE

ABSTRACT

BEHAVIOUR OF HIGH-STRENGTH CONCRETE COLUMNS
UNDER ECCENTRIC COMPRESSION - TIED COLUMNS

CANBAY, Erdem

M.S., Department of Civil Engineering

Supervisor: Assoc. Prof. Dr. Güney Özcebe

August, 1995, 99 pages

In this study, the behaviour of high strength concrete square columns under eccentric compressive loading was investigated. Within this scope, six high strength concrete column specimens were tested under eccentric compression. The variable parameters were presence of lateral confinement, tie spacing and cross-tie efficiency. Effect of confinement on column strength and column ductility were discussed with the obtained test results. Furthermore, the experimental response was compared with the load-strain, moment-curvature and interaction diagrams obtained from concrete models used in this study. The results indicate that:

- HSC columns showed extremely brittle behavior unless confined by transverse reinforcement.
- Cross-ties with 90° bend at one end and 135° at the other end was as effective as the one with 135° bend at both ends.

- A mechanical ratio, (defined as volumetric ratio of lateral reinforcement times yield strength of ties divided by strength of concrete), of 7% could not achieve any ductility gain. It prevented only the explosive type of failure of the concrete column. This column showed a strength enhancement of approximately 15% compared with the unconfined reference specimen. No improvement was observed at the post peak region.
- Minimum requirements in TS500 provision for the confining steel was not sufficient for HSC.
- The statement in TS500 (12.3.3) might be revised as follows: "tie spacing should be less than or equal to 12 diameter of longitudinal reinforcement and 200 mm. For specified concrete compressive strengths in excess of 50 MPa, the tie spacing determined above shall be multiplied by 0.75."
- Among three models used in the analytical study, the agreement of the Nagashima concrete model [21] with the experimental observations was satisfactory.
- The mechanical ratio was a very important variable. One way of increasing this ratio was increasing the yield strength of the lateral reinforcement, that could keep the mechanical ratio as high as required with realisable tie spacing. Therefore, with high strength concrete, high strength steel should be used.

Keywords: High Strength Concrete, Confinement, Eccentric Compressive Load, Strength Enhancement, Ductility Enhancement, Cross-tie Efficiency

Science Code:

ÖZ

EKSENTRİK YÜKLÜ YÜKSEK DAYANIMLI BETON KOLONLARIN DAVRANIŞI - ETRİYELİ KOLONLAR

CANBAY, Erdem

Yüksek Lisans Tezi, İnşaat Mühendisliği Bölümü

Tez Yöneticisi: Doç. Dr. Güney Özcebe

Ağustos, 1995, 99 sayfa

Bu tezde, yüksek dayanımlı kare kolonların eksentrik basınç yükü altında davranışları incelenmiştir. Bu amaçla, altı adet yüksek dayanımlı beton (YDB) kolon numunesi eksentrik basınç altında denenmiştir. Deney elemanlarının değişken parametreleri etriye oranı, etriye aralığı ve çiroz etriyelerin yeterliliği idi. Deneyden elde edilen sonuçlarla etriyelerin kolon dayanımı ve sünekliği üzerindeki etkileri tartışılmıştır. Ayrıca, deneysel davranış bu çalışmada kullanılan beton modellerinden elde edilen yük-birim deformasyon, moment-eğrilik ve karşılıklı etki diyagramlarıyla karşılaştırılmıştır. Bu çalışma sonucunda aşağıdaki sonuçlara varılmıştır:

- YDB etriyelerle sarılmadığı sürece çok gevrek bir davranış göstermektedir.
- Bir ucu 90° öbür ucu 135° bükülen çiroz etriyeler iki ucu da 135° bükülen etriyelerle aynı etkiyi sağlayabilmişlerdir.

- Yüzde 7'lik bir mekanik donatı oranı (etriye hacimsel donatı oranı çarpı etriye akma dayanımı bölü beton dayanımı) süneklik artışı gösterememiştir. Sadece beton kolonun patlama şeklindeki kırılması engelenmiştir. Bu kolon etriyesiz referans kolonuna göre yüzde 15'lik bir dayanım artışı göstermiştir. Pik sonrası davranışta herhangi bir iyileşme gözlenmemiştir.
- TS500'deki etriye ile ilgili minimum şartlar YDB için yeterli değildir.
- TS500'deki 12.3.3 şartı şu şekilde revizyondan geçirilebilir: "etriye aralığı 12 boyuna donatı çapından ve 200 mm den az veya eşit olmalıdır. Beton dayanımı 50 MPa üzerinde ise yukarıdaki şartlara göre belirlenen etriye aralığı 0.75 ile çarpılmalıdır."
- Bu çalışmada kullanılan beton modelleri arasında Nagashima modeli [21] deneysel davranışla yeterli bir uyuşma göstermiştir.
- Mekanik donatı oranı önemli bir değişkendir. Bu oranı arttırmanın bir yolu kullanılan etriyenin akma dayanımını arttırmaktır. Böylece gerekli mekanik donatı oranı gerçekleştirilebilir (uygulanabilir) etriye aralıklarıyla sağlanabilir. Bu yüzden yüksek dayanımlı betonla birlikte yüksek dayanımlı donatı kullanılmalıdır.

Anahtar Kelimeler: Yüksek Dayanımlı Beton, Etriye, Eksentrik Basınç Yükü, Dayanım Artışı, Süneklik Artışı, Çiroz Etriyelerin Etkisi.

Bilim Dalı Sayısal Kodu:

dedicated to my wife Feyhan ...

ACKNOWLEDGEMENTS

This study was conducted under the supervision of Assoc. Prof. Dr. Güney Özcebe. I would like to convey my sincere appreciation to him for his helpful guidance and endless encouragement throughout this thesis.

I owe special thanks to Prof. Dr. Uğur Ersoy, Prof. Dr. Tuğrul Tankut and Prof. Ş. Muvaffak Üzümeri for their valuable recommendations and continuous concerns.

The financial supports from the Scientific and Technical Research Council of Turkey (INTAG-Research Project No:502) and Middle East Technical University (AFP-Research Project No:91-03-03-01) are gratefully acknowledged.

I would like to extend my thanks to the structural mechanics laboratory staff for their assistance during the experiments.

I also would like to thank to my mother, father, sister and brother for their support during this study.

Finally I would like to give my heartfelt thanks to my wife for her continuous support, help and endless love.

TABLE OF CONTENTS

LIST OF TABLES

TABLE

LIST OF FIGURES

FIGURES

LIST OF SYMBOLS

A_c	cross-sectional area of the column
A_s	area of lateral steel
b	the center-to-center distance of perimeter tie
b_d	diameter of transverse reinforcement
E	modulus of elasticity
f_c	concrete cylinder strength
f_y	yield strength of the bars
f_{yt}	yield strength of transverse reinforcement
f_{ult}	ultimate strength of steel
K_s	the ratio of confined strength to unconfined strength of concrete
M	moment
N	normal force
N_{test}	normal force carried by column
$N_{o,c}$	normal force carried by concrete
$N_{o,s}$	normal force carried by steel
s	tie spacing
ε_m	strain at peak load
ε_{sh}	strain at the beginning of strain hardening
ε_y	strain at yielding of steel
φ	curvature
μ	poisson's ratio
ρ	ratio of longitudinal bars
ρ_s	volumetric ratio of transverse reinforcement
σ_c	stress in concrete

CHAPTER I

INTRODUCTION

1.1. General

Concrete is the most widely used man-made construction material. The use of concrete dates back at least 9000 years. Concrete became popular in 19th century and it was improved considerably since then. The discovery of silica fume as an additive to concrete, in combination with the development of high-performance plasticizers, made it relatively easy to produce High Strength Concrete, HSC. In the last ten or twenty years there have been great strides in the development and application of HSC [1,2]. The term high strength concrete has changed its meaning over the years. In the 1950's, concrete with a standard cylinder (150x300 mm) compressive strength of 35 N/mm^2 (MPa) was considered high strength in the USA. In the 1960's commercial usage of 40-50 MPa concrete was achieved. In the early 1970's concrete strength reached 65 MPa. Today, concrete with design strengths over 80 MPa are being considered for applications in cast-in-place buildings and prestressed concrete members [3,4].

In recent years, the applications of HSC have increased and HSC has been used in many parts of the world. The growth has been possible as a result of recent developments in material technology and a demand for higher-strength

concrete. There is a very large field of application for HSC. There are both technical and economical advantages of using HSC in structures. The use of HSC in tall buildings has an important reason, which is the wish to build high, but in the mean time to keep the effective floor area as large as possible. Columns of high-rise structures have been the largest application of HSC in buildings. One of the drawbacks of normal strength concrete construction has been that the sizes of the columns end up substantially larger than those for an all steel buildings thereby greatly reducing the usable area on floors. Thus, use of HSC can avoid oversize columns on the lower floors, and increases rentable floor space [5]. Because of its higher modulus of elasticity, deflections of tall, slender buildings can also be reduced. In highway bridge applications, the use of HSC can result in greater compressive strength per unit cost. Its high modulus of elasticity results in reduced deflections. HSC has been used in many precast prestressed bridge girders, which would allow for the use of longer spans, which in turn would decrease the number of piers required for support and reduced cost. Another large application area for HSC is the offshore structures. The important requirement is not only the very high strength, but also rather a high durability, a good workability and a high erection speed. Some other examples can be given as highway pavements, thin arch dams, piles for marine foundations, prestressed concrete poles, safe deposits, temporary underwater foundations, precast elements, etc. Some examples for the use of HSC in buildings and bridges are given in Table 1.1 and Table 1.2 respectively.

Table 1.1 Buildings with high strength concrete

Building	*Location*	*Year**	*Total stories*	*Maximum design concrete strength MPa*
Pacific Park Plaza	Emeryville CA	1983	30	45
S.E. Financial Center	Miami	1982	53	48
Petrocanada Building	Calgary	1982	34	50
Lake Point Tower	Chicago	1965	70	52
1130 S. Michigan Ave.	Chicago			52
Texas Commerce Tower	Houston	1981	75	52
Helmsley Palace Hotel	New York	1978	53	55
Trump Tower	New York		68	55
City Center Project	Minneapolis	1981	52	55
Collins Place	Melbourne		44	55
Larimer Place Condominiums	Denver	1980	31	55
499 Park Avenue	New York		27	59
Royal Bank Plaza	Toronto	1975	43	61
Richmond-Adelaide Centre	Toronto	1978	33	61
Midcontinental Plaza	Chicago	1972	50	62
Frontier Towers	Chicago	1973	55	62
Water Tower Place	Chicago	1975	79	62
River Plaza	Chicago	1976	56	62+
Chicago Mercantile Exchange	Chicago	1982	40	62++
Columbia Center	Seattle	1983	76	66
Interfirst Plaza	Dallas	1983	72	69
Barnett Plaza in Tampa	Florida	1985	42	41
900 N. Mich. Annex	Chicago	1986	15	97
South Wacker Tower	Chicago	1989	79	83
Grande Arche de la Defense	Paris	1988		65
Two Union Square	Seattle	1989	58	115
Pacific First Center	Seattle	1989	44	115
311 South Wacker Tower	Chicago	1989	68	83
Gateway Tower	Seattle	1989	62	94
530 Collins Stret	Melbourne	1990	39	60
Bourke Place	Melbourne	1990	55	60
One Peachtree Center	Melbourne	1991	+++	83
Melbourne Central Tower	Melbourne	1991	55	65
The Nations Bank Tower	North Carolina	1992	60	55

* Year in which HSC was cast

\+ Two experimental columns of 76 MPa strength were included

++ Two experimental columns of 97 MPa strength were included

+++ 257 m

Table 1.2 Bridges with high strength concrete

Bridge	*Location*	*Year*	*Maximum span (m)*	*Maximum design concrete strength concrete*
Willows Bridge	Toronto	1967	48	41
Houston Ship Canal	Texas	1981	229	41
San Diego to Coronado	California	1969	43	41 L*
Linn Cove Viaduct	North Carolina	1979	54	41
Pasco-Kennewick Intercity	Washington	1978	299	41
Coweman River Bridges	Washington		45	48
Huntington to Proctorville	W. Va. to Ohio	1984	274	55
Nitta Highway Bridge	Japan	1968	30	59
Kaminoshima Highway Bridge	Japan	1970	86	59
Tower Road Bridge	Washington	1981	49	62
Fukamitsu Highway Bridge	Japan	1974	26	69
Ootanabe Railway Bridge	Japan	1973	24	79
Akkagawa Railway Bridge	Japan	1976	46	79
Kylesku Bridge	Scotland	1978	79	53
Deutzer Bridge	W. Germany	1978	185	69*
Parrot Ferry Bridge	California	1979	195	43*
Pont de Tricastin	France		142.4	30*
Ottmarsheim	France	1979	172	30*
Selbjorn Bridge	Norway	1977	212	40
Pont du Pertuiset	France	1988	110	65
Pont de Joigny	France	1988		60
Arc sur la Rance	France	1989		60
Giske	Norway	1989	52	55
Sandhornoya	Norway	1989	154	55*
Boknasundet	Norway	1990	190	60*
Helgelandsbrua	Norway	1990	425	65
Chesapeake&Delaware Canal	Delaware	1991	229	40

* Lightweight concrete

High Strength Concrete offers much more than its high strength alone. There are some additional benefits, such as:

- High early strength : When the water-cement ratio is reduced, the relative gain of strength is also accelerated. Therefore, HSC shows a higher rate of strength gain at early ages as compared to lower-strength concrete. This property allows early stripping of the forms. Columns and girders can easily be stripped at three days thereby enabling the construction to proceed at the rate of approximately two floors per week. Hence, the speed of construction rivals the speed of steel construction .

- High plasticty of the concrete mixture : HSC will in many cases be very suitable for pumping. HSC is likely to have a high cement content and small maximum size aggregate - both factors which facilitate concrete pumping. The high plasticity of the concrete mix during casting makes compaction nearly superfluous, which results not only into a reduction of labour costs, but also leads to saving in terms of energy, time and equipment.

- Resistance against abrasion, wear and tear : In cold climates, HSC is of special interest for road pavements, since this material provides excellent resistance to wear from studded tyres. Norwegians have already been recognized the high resistance against mechanical abrasion and erosion. The cars equipped with tyres having small steel studs to improve the friction between the tyre and the road and to improve driver control during the winter season. The wearing effect on ordinary asphalt pavement is enormous. But, HSC in the order of 100-120 MPa has the same wearing resistance as massive granite.

- Higher resistance against the penetration of chemicals : HSC provides high resistance against chemicals, like chlorides and salt, and gives good protection to the reinforcement because of its low porosity. The low permeability of HSC against chemicals is a very favourable property with regard to durability in general.

- High modulus of elasticity and stiffness : The modulus of elasticity of concrete is closely related to the properties of the cement paste, the stiffness of the selected aggregates, and also the method of determining the modulus. It has been shown that the modulus of elasticity increases with the concrete strength. The increase of modulus of elasticity for higher strength concretes results in greater axial stiffness of the columns and consequently, better behaviour under lateral loads. The higher modulus of elasticity of HSC reduces the short-term axial shortening of column both due to the gravity loads and wind forces.

- Lower creep : The maximum specific creep is less for HSC than for lower-strength concretes loaded at the same age. Lower creep values has a beneficial effect in reducing the differential shortening between interior and exterior vertical load-carrying members.

- Economical Benefit : The economical advantages of using HSC in the columns of high-rise buildings have been clearly demonstrated by applications in many cities. It has been shown by studies that the cost of a column for a given load on a tall building is substantially lower in HSC than it is in lower strength concrete.

1.2. Research Needs

Although HSC is often considered a relatively new material, it is widely used all around the world. As with many developments of new materials research, data supporting the growth has also increased. During the last decade a considerable amount of research has been carried out on HSC. However, information is still needed to fully use the advantages of HSC and to affirm its capabilities.

High concrete strengths are beyond the scope of most national and international standards. Design equations which are based on tests and surveys of members for which the concrete strength was less than approximately 40 MPa. Verification is required that these design equations are applicable to higher-strength concretes. At the first the codes have to be extended to the higher concrete classes. Future programmes have to give priority to providing data for HSC in national and international design codes.

Present code provisions are often used without any additional precautions for safety in construction projects involving HSC. The parameters defining the requirements for lateral confining reinforcement in current codes are based on the results of tests done on normal strength reinforcement concrete members. Therefore, current code requirements may not be adequate nor safe for HSC members. Configuration of reinforcement and the influence of the material strength on confinement should be studied [1,2,4,6,7,8].

1.3. Object and Scope

The objective of this study is to investigate the effect of ties on the strength and the ductility characteristics of high strength concrete columns. In an earlier test conducted in Middle East Technical University, METU, spiral columns were studied [41]. Thus, square columns were chosen to study in this experimental program. Purposely six column specimens with different confinement amounts were prepared and tested under eccentrically applied axial load.

Columns in reinforced concrete frames are rarely loaded in a statically determinate manner, but the isolated and statically loaded column is helpful as a starting point for discussion [37,39].

The scope of this study includes:

- Review of previous researches,
- Design, preparation and testing of six high strength concrete column specimens,
- Evaluation of the data gathered during the tests,
- Application of the analytical models developed both for normal strength concrete and high strength concrete to test specimens,
- Comparison of the test results with the analytical predictions,
- Presentation of the results.

CHAPTER II

LITERATURE SURVEY

There are many researches carried out on the normal strength concrete columns. The behaviour of these columns is well understood and also mechanical properties of NSC are deeply studied. In recent years there have been also many researches on HSC.

Research on the effect of lateral reinforcement in concrete columns has begun with two papers published by King in 1946 [9]. Since then, all researchers, have agreed that the presence of closely spaced rectangular ties greatly enhances the ductility of concrete columns. However, until 1970 there was no consistency in the results of the several investigations carried out for strength increase due to the presence of lateral ties. These brief conclusions cover the investigations until 1970's. Literature survey concerns the period between 1970 and today.

Burdette and Hilsdorf [9] (1971) concluded on 5 in. by 5 in. by 25 in. prism with lateral reinforcement in the form of steel angles at the prism corners and conventional rectangular ties that the presence of closely spaced rectangular ties causes an appreciable increase in column ductility. This enhancement of column behavior was of more practical significance than the relatively small strength increase

due to ties. In addition, they concluded that the presence of cross bars welded to the ties to provide added flexural rigidity results in significantly increased column ductility, and the use of cross bars in each direction caused a significantly greater strength increase.

Kent and Park [14] (1971) proposed a stress-strain curve for unconfined and confined concrete. Experimental basis of this study was the work of Soliman and Yu (44), Roy and Sozen (45) and Bertero and Felippa (46). They represented the curve by a second degree of parabola up to maximum stress, a linear falling branch and a horizontal linear portion with stress constant at 0.2 of the maximum stress. The ascending portion of the curve depends on concrete strength only. The slope of the linear falling branch was found to depend on the concrete cylinder strength, the ratio of width of confined concrete to spacing of hoops and the ratio of volume of hoop steel to volume of concrete core. They determined with the use of stress block parameter the moment-curvature characteristics and the ductility of flexural members.

Sheikh and Uzumeri [10] (1980) performed an experimental program involving short concrete columns with complex tie arrangements. There was in total twenty-four (305x305x1960 mm) columns tested under monotonic axial compression. Some of the conclusions are listed below:

- Concrete, when confined with rectangular ties and well-distributed longitudinal steel, exhibits a very significant strength gain, as well as increased ductility.

- It appears that the area of the effectively confined concrete is less than the nominal core area bounded by the center line of the perimeter tie, and is determined by the

distribution of the longitudinal steel the resulting tie configuration, and the spacing of ties.

Park, Priestley and Gill [11] (1982) tested four nearly full size reinforced concrete columns with a 550 mm square cross section, various axial load levels, and various quantities of rectangular hoops placed according to the provisions on the draft New Zealand Concrete Design Code. They observed high concrete compressive strains at the maximum moment, which cause that the flexural strength of the columns to exceed the predicted theoretical values based on ACI column design charts. They proposed a modified version of Kent and Park stress-strain model for confined concrete. This model and Sheikh and Uzumeri model gave the closest agreement with the experimental moments.

Sheikh [12] (1982) compared the results of various models for the stress-strain relation of concrete confined by ties. He concluded that in addition to the commonly acknowledged variables such as the amount of lateral reinforcement and steel strength, two other variables, namely the distribution of the longitudinal steel around the core perimeter and the resulting tie configuration, and the spacing of ties, play important roles in determining the behaviour of the confined concrete. He observed that better distribution of steel and closer spacing of ties along the column longitudinal axis (for the same amount of reinforcement) result in higher concrete strength and ductility.

Sheikh and Uzumeri [13] (1982) developed an analytical model for the confinement mechanisms in tied columns. They calculated the strength of the confined concrete by using the concept of the effectively confined concrete area within the

nominal concrete core. The area of the effectively confined concrete was determined by the tie spacing, the distribution of longitudinal steel around the core perimeter and the resulting tie configuration. They also examined Building Code requirements for confinement and concluded that in certain circumstances the Codes provisions may be unsafe, while in others they may be unnecessarily conservative.

Fafitis and Shah [15] (1985) proposed analytical expressions for the stress-strain curves of confined and unconfined NSC and HSC both for square and circular sections. Proposed model gave satisfactorily good results. They concluded that:

- The increased amount of lateral reinforcement required by ACI code for higher compressive strength concrete compensates the inherently poorer efficiency of confinement in HSC. However, this may not be true for concrete strength of greater than 62 MPa.

- The rate of drop in the moment capacity of the column after the first peak is higher for higher compressive strength concrete.

- The moment-curvature curve of columns subjected to monotonically increasing lateral force can be approximately considered as an envelope to the response of the columns subjected to the cyclic lateral loading.

Young , Nour and Nawy [16] (1988) reported the empirical results of a test program studying the effects of rectilinear confinement in HSC subjected to a monotonically increasing compressive axial load. The stress-strain behaviour was

studied with respect to the effects of the volumetric ratio of lateral ties, the concrete cover, and the distribution of the longitudinal steel around the core perimeter. They observed that:

- The lateral steel confinement was not as effective as in low and normal strength concrete.

- Columns with only four longitudinal bars at the corners exhibited much less ductility than columns with the same volumetric ratio of lateral steel but with eight longitudinal bars.

- For effective rectilinear confinement in HSC the lateral tie spacing must be less than the lateral dimension of the specimen, not less than eight longitudinal bars distributed along the perimeter of the specimen.

Saatcioglu and Razvi [17] (1992) proposed an analytical model to construct a stress-strain relationship for confined concrete. The analytical procedure was based on equivalent uniform confinement pressure generated by the reinforcement cage. The results of comparisons, which included concentric and eccentric loading, as well as slow and fast strain rates, on circular, square and rectangular columns, with spiral and rectilinear reinforcements, as well as welded wire fabric, indicated good agreement.

Galeota, Giammattes and Marino [18] (1992) presented the results of an experimental investigation on the structural behaviour of HSC, confined by rectilinear steel ties and subjected to generalised compression loads. Tests were performed on 40

prismatic HSC specimens by 150x150x450 mm in dimensions with only rectilinear lateral steel ties, but no longitudinal reinforcement, and no cover was provided. The following conclusions were drawn from this study:

- The compressive strength, strain at maximum stress and ductility of HSC core specimens confined by rectilinear steel ties, all increased as the amount of confinement degree increased. However, the rate of increase was lower than for NSC with similar confinement degrees.

- The proposed stress-strain curve agreed accurately with the experimental stress-strain curves.

- It was found based on the previous model that properly reinforced sections made of HSC exhibit ductile structural response, and that the amount of confinement has a great effect on large strains or curvatures.

Hatanaka and Tanigawa [19] (1992) conducted a series of triaxial compression tests of normal and high strength concrete cylinders, 10 cm in diameter and 10 cm in height, carried out by using a steel ring confinement. In this study the earlier stress-strain model, proposed by authors, for concrete under triaxial compression is extended to be applicable to the concrete of higher compressive strength up to 100 MPa and under higher confining pressure up to 5 MPa. They also concluded that in order to keep concrete non-softening type or to maintain the stress as large as uniaxial compression strength σ_0, at least $\sigma_0/20$ lateral pressure ${}_R\sigma_L$ is required (${}_R\sigma_L \geq \sigma_0/20$).

Itakura and Yagenji [20] (1992) studied the effects of longitudinal steel bars, spiral reinforcement and tie bars on the uniaxial compressive behaviours of high-strength reinforced concrete columns. Tests were carried out on nine-teen 500 mm and five 750 mm tall and 218 mm square columns until failure. The results of experimental work were summarised as follows:

- Tie bars tremendously enhanced the core concrete strength until failure.

- Tie bars having 135° hooks with six-diameter extension length anchored in the core concrete were not effective compared to that with ten-diameter extension length.

- The lateral reinforcement does not only enhance the axial load carrying capacity of core concrete due to its confining effect, but also absorbs similar energy to that of longitudinal reinforcement.

Nagashima, Sugano, Kimura and Ichikawa [21] (1992) conducted an experimental program involving HSC and ultra-high-strength concrete (UHSC) square columns with complex tie arrangements. Specimens were 716 mm long prisms with a 225 mm square cross section. They proposed an analytical model of the stress-strain curve for concrete strength up to 118 MPa. They used the Sheikh & Uzumeri model with a simplification to calculate the reduction factor for effective capacity of lateral reinforcement. Following conclusions were drawn:

- For columns with UHSC of 118 MPa, the capacity of lateral reinforcement normalised by strength of plain concrete ($A_s/(b\ s)*f_{yh}/f_c"$) higher than 0.18

prevented a sudden failure after the maximum strength was reached and improved compression ductility when the double cross-tie configuration was used.

- The strength of longitudinal steel had little effect on the stress-strain relation of the confined concrete.

- The maximum strength of confined concrete was independent of the number of longitudinal bars when the same tie configuration was used.

- The maximum stress enhancement of confined concrete from plain concrete was independent of the concrete strength and was proportional to the square root of the effective lateral confinement capacity.

- The compression ductility of confined concrete was directly proportional to the capacity of lateral steel and inversely proportional to the concrete strength.

Collins, Mitchell and MacGregor [22] (1993) examined HSC from various aspects. They highlighted some aspects of structural design where traditional procedures may need to be modified to account for the different characteristics of HSC. They investigated the stress-strain response, capacity of columns, minimum reinforcement and ductility of tension and flexural members and shear strength of HSC.

Nishiyama, Fukushima, Watanabe and Muguruma [23] (1993) carried out axial loading tests on 250x250x750 mm reinforced concrete prisms. The cylinder compressive strength was approximately 110 MPa and the yield strength of confining

reinforcement was 400 and 800 MPa. They concluded that confining reinforcement with 800 MPa yield strength and volumetric ratio of more than 4% should be required to prevent HSC prisms from brittle axial compression failure. They observed also that after spalling off cover concrete specimen with cover concrete showed almost the same stress-strain relationship as the specimen without cover concrete. In the test specimen with high-strength steel the peripheral hoops remained elastic at the peak-stress while the inner sub-hoops yielded.

Al-Hussaini, Regan, Xue and Ramdane [24] (1993) conducted HSC column tests to extend basic design rules to cover higher concrete strength. All eight columns were 2.0 m long with 250 mm square cross section and with concrete cube strengths from 112 to 144 MPa. The columns developed strengths substantially in agreement with those predicted if the British code equations are extrapolated to the significantly higher concrete strengths involved. They also observed that although the load capacities of all the specimens were satisfactory the code's minimum links were insufficient either to prevent the buckling of main bars between them or to give the columns any ductility in compression.

Azizinamini and Kuska [25] (1993) conducted a combined experimental and analytical investigation to study the ductility of square HSC columns subjected to loads simulating earthquake effects. Some necessary conclusions are listed below:

- The ductility of HSC columns increases as the level of axial load decreases and as the volume of transverse reinforcement increases.

- Square HSC (f_c' exceeding 69 MPa) columns with applied axial load levels below 20% of the column's axial load capacity and designed based on seismic provisions of ACI-318-89 building code possess adequate curvature and displacement ductilities.

- For square HSC columns ACI-318-89 procedures over estimate the flexural capacity of column section. Therefore, they suggested to reduce the stress intensity of equivalent rectangular compression block to $0.6f_c'$ from $0.85f_c'$ linearly to calculate the nominal moment capacity of HSC columns with axial loads ranging up to 30% of the column's axial capacity.

Cusson and Paultre [26,29] (1993) carried out an experimental study, to understand the complex mechanism of confinement, on 27 large-scale HSC columns confined by rectangular ties tested under concentric monotonic loading. They concluded that longitudinal weakness planes, which are caused by the dense steel cage between the concrete core and the concrete cover, separated the concrete cover prematurely from the concrete core at high axial loads, that prevents the specimen from reaching its expected maximum load. It was observed that HSC columns exhibit less ductile behaviour compared to equally reinforced NSC columns. However, irrespective of the concrete strength, the utilisation of a better tie configuration, that produce uniform and large confining pressure, improves moderately the strength and the ductility of confined concrete. The failure of HSC columns is characterised by the formation of inclined shear sliding surfaces, separating the concrete core into two wedges. The inclination of the shear sliding plane with the vertical axis varies from 25 ° for low-confined to 45° for highly confined specimens. They developed a theoretical stress-strain model for confined HSC. For the ascending part they used the Popovics

curve, for the descending part they modified Fafatis and Shas's curve and for the confinement effectiveness coefficient they used Sheikh and Uzumeri equation modified by Mander et al.

Muguruma, Nishiyama and Watanabe [27] (1993) proposed a stress-strain idealisation for 20 to 120 MPa in compressive strength. They extended the idealisation for application to confined concrete. Flexural analysis, which incorporates the idealisation, was conducted on reinforced concrete column sections with concrete of 130 MPa in compressive strength and confined by high strength transverse steel. The theoretical curve predicted the experimental curve well with respect to the moment capacities and the general shape of the loops until the rotation angle of 0.02 rad.

Saatcioglu and Razvi [28] (1994) experimentally investigated the strength and deformability of HSC columns. They tested 12 specimens consist of square columns with 250 mm cross-sectional dimension, and 1.5 m height. They reached the following conclusions:

- HSC columns show extremely brittle behaviour unless properly confined by transverse reinforcement.

- HSC columns require significantly higher volumetric ratio of confinement reinforcement than those typically used for NSC columns. There is experimental evidence that the extra steel requirement may be offset by the use of higher grade confinement reinforcement. The columns with $\rho_s f_{yt}/f_c'$ ratios of 14% and 22%

produced favourable deformation characteristics for columns with 12-bar and 8-bar arrangements, respectively.

- Unconfined strength of concrete in columns was found to be approximately 90% of the strength determined by cylinder tests. However, columns with confinement reinforcement experienced premature failure of the cover. Cover failure was in the form of instability of the shell, and occurred at lower compressive strains than those associated with concrete crushing.

Razvi and Saatcioglu [30] (1994) also investigated the strength and deformability of confined high-strength concrete columns based on available experimental data. They evaluated up to 250 columns, tested either under monotonically increasing concentric loading or reversed lateral loading. Additional conclusions are listed below:

- High-strength steel of up to 1000 MPa is effective in confining HSC columns. However, when excess volumetric ratio of steel over and above the practical range is provided, the beneficial effect of high-strength steel may not be seen, especially under low levels of axial load.

- Deformability of HSC columns decreases with axial compression. However, it is possible to obtain high deformabilities in highly compressed HSC columns, when either the volumetric ratio and/or the strength of confinement reinforcement is increased.

- Reduction in the spacing and spacing of laterally supported longitudinal reinforcement improves both strength and deformability of confined HSC columns.

- Circular spirals are more effective than rectilinear ties.

- They proposed that until the characteristics of the cover concrete are well established, it may be prudent to base the concentric capacity calculations on the core area rather than the total cross-sectional area of columns.

CHAPTER III

EXPERIMENTAL PROGRAM

3.1. General

In this experimental study six reinforced concrete columns were tested under eccentric compressive load. Except one column, all specimens were provided with lateral reinforcement. One column specimen had no lateral reinforcement in the test region. The purpose of testing this specimen was to determine the unconfined capacity of the test columns experimentally. Following parameters were considered in the experimental study:

- Tie spacing,
- Tie arrangement.

Test specimens were named as D10-135, L8-75 etc. The first letter shows the tie configuration of the specimens. All specimens had an outer tie confining the four corners longitudinal bars. The letter "D" states for an inner diagonal tie confining the four bars at the midsides of the column section. The letter "S" and "L" are for two perpendicular cross ties confining the facing midside bars. The former had a standard hook with bend of 135° at both ends. The latter had a standard hook with bend of 135° at one end and a standard hook with a bend of 90° at the other end. Again, the first

number is for the diameter of the lateral ties. Finally, the last part of the notation indicates the tie spacing. The unconfined specimen is named as Reference.

3.2. Materials

3.2.1. Concrete

Concrete was produced in the mechanical laboratory of the METU. The planned compressive cylinder strength was 75 MPa. To increase the strength of concrete up to 75 MPa, the water/(cement+silica) ratio was reduced to 0.18. Table 3.1 shows the mix design of concrete. Mix design values are given by weight for $1m^3$ concrete and used for both batches.

Great attention was given to curing. Proper curing is almost as important as the proportioning of the mix, because the final strength of concrete is greatly influenced by curing. Curing was done by covering the specimens with wet cotton burlap which kept the concrete moist and as near as possible to the ideal temperature for chemical hydration.

In order to determine the concrete strength, 15 standard cylinder test specimens were taken from each batch. The test cylinders were 15 cm in diameter and 30 cm in height. The test cylinders were kept under the same moist curing conditions as the column specimens. Figure 3.1 shows the strength gain in time for concrete of both batches. Three cylinders were tested to obtain each point on the figure.

Table 3.1 Mix Design of $1m^3$ Concrete

	Weight (kg)	Proportions by weight (%)
Cement	600	22.98
0-3 Aggregate	530	20.30
3-7 Aggregate	370	14.17
7-15 Aggregate	830	31.78
Silica fume	110	4.21
Superplasticizer Melment L10/33	46.2	1.77
Water	125	4.79
Total	2611.2	100

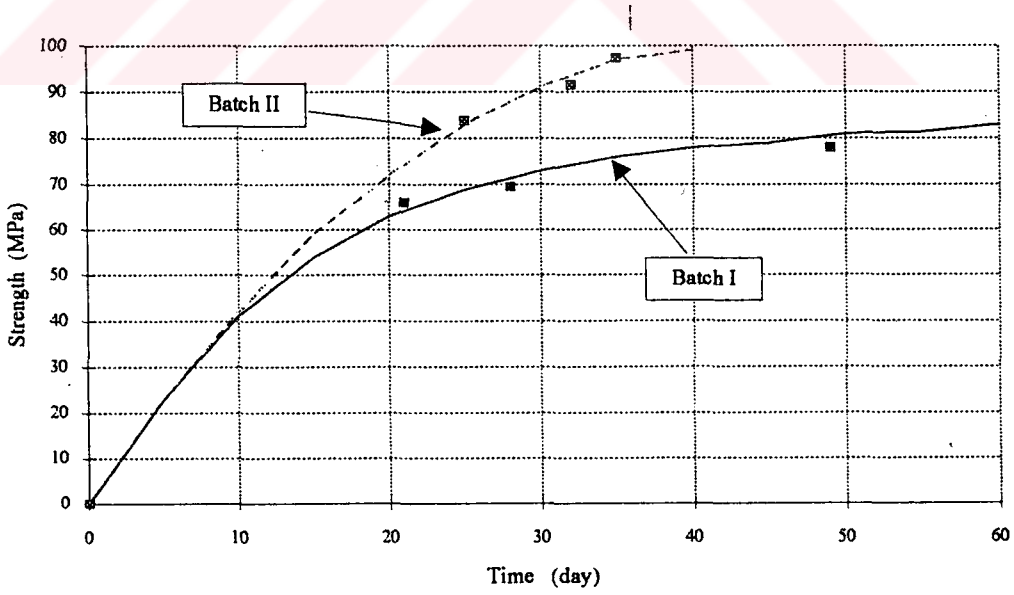

Figure 3.1 Strength gain in time of the concrete

3.2.2. Steel

In each specimen eight longitudinal steels plain bars were used. Longitudinal steel was 14 mm in diameter. The longitudinal reinforcement of all specimens were prepared from the same batch. Three test coupons were randomly taken to determine stress-strain relationship of steel used. The coupons were tested in tension. The strains were measured over a gauge length of 50 mm. The diameter of the bar in test region was reduced precisely in order to obtain the yielding within the test region. Elongation readings were taken over the gauge length from which the average strains were calculated. Simultaneously, load readings were taken from which the average stresses imposed on the steel were obtained. After the manipulation of the data the stress versus strain curve was drawn. From the graph, the yield strength, f_y, the yield strain, ε_y, strain at the beginning of strain hardening, ε_{sh}, and modulus of elasticity, E, were obtained. A typical σ-ε curve is given for ∅14 bars in Fig.3.2.

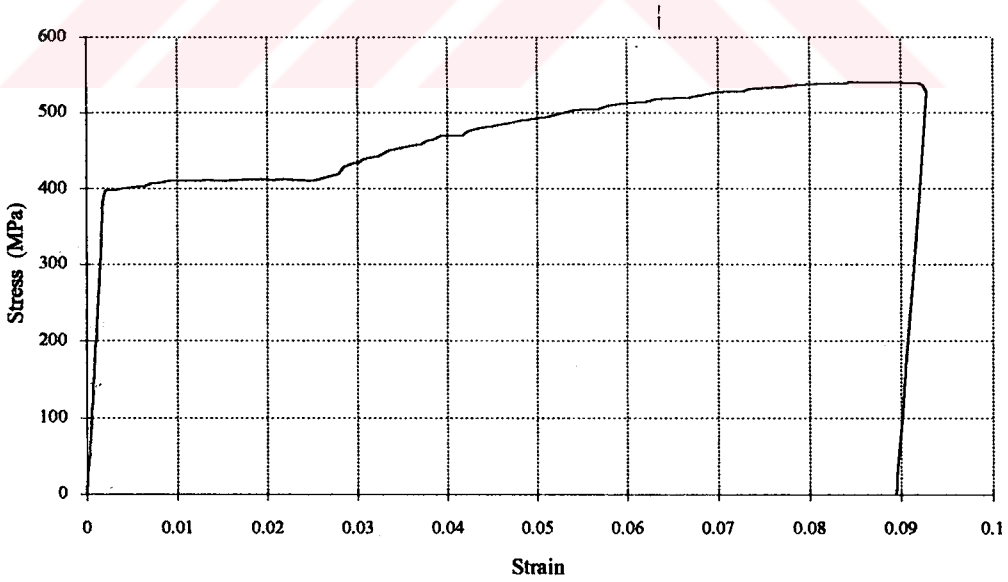

Figure 3.2 Stress - Strain Curve of Steel ∅14

Two different sizes of steel were used to prepare ties. 8 mm diameter plain bars were used to fabricate the reinforcement of specimens D8-75, S8-75, L8-75 and D8-120. Specimen D10-135 had ties made of 10 mm plain bars. Fig.3.3 and Fig.3.4 shows the stress-strain curves of ∅8 and ∅10 bars respectively.

Typical properties of bars are listed in Table 3.2. Ductility of the bars used in tests was so high that elongation of the bar exceeded the maximum opening of the gauge legs. For this reason, gauge was taken out at a strain approximately 0.1 and test was continued without strain measurement. In the table, the yield strength, f_y , yield strain, ε_y, strain at the beginning of strain hardening, ε_{sh}, ultimate strength, f_{ult}, and modulus of elasticity, E, were given.

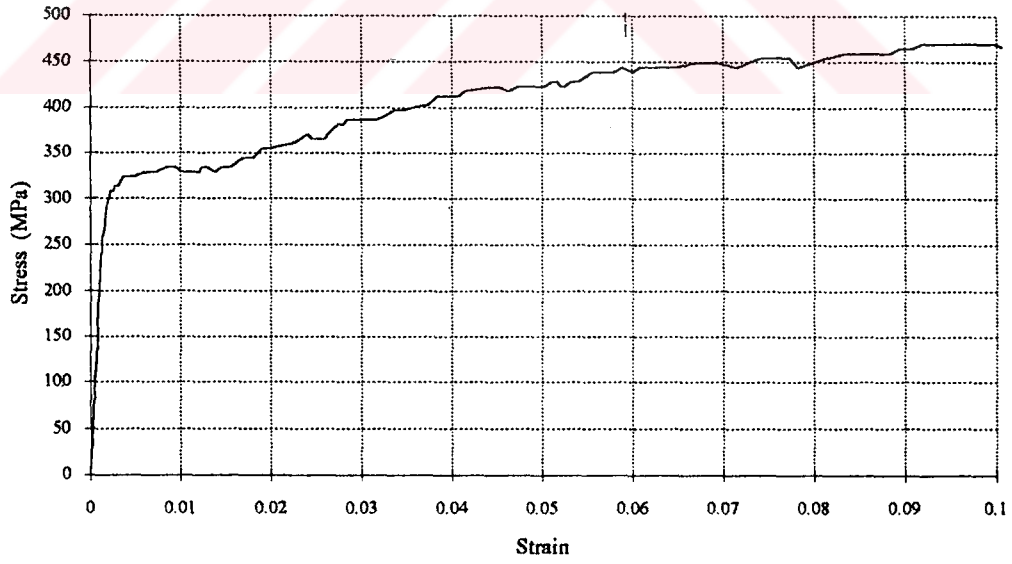

Figure 3.3 Stress - Strain Curve of Steel ∅8

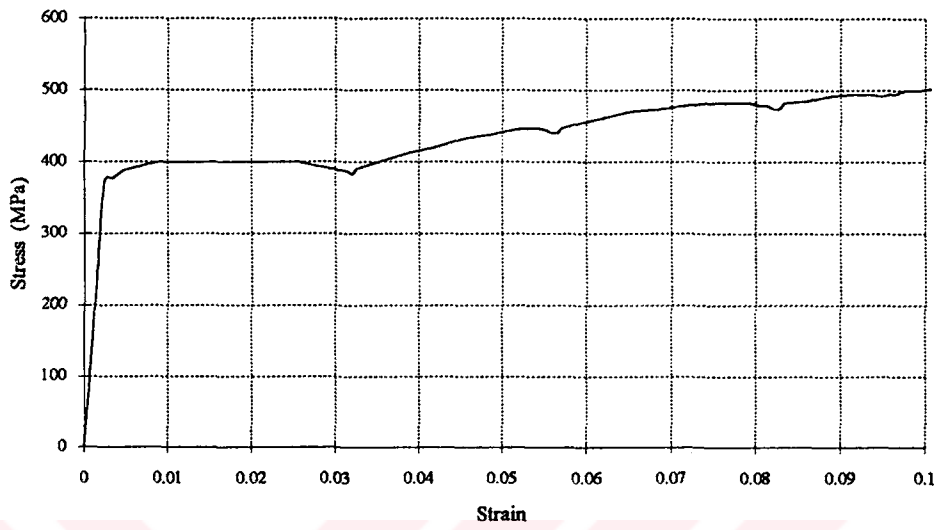

Figure 3.4 Stress - Strain Curve of Steel ∅10

Table 3.2 Typical properties of the steel

	f_y (MPa)	ε_y	ε_{sh}	f_{ult} (MPa)	E (MPa)
∅8	323	0.0016	0.015	475	~200000
∅10	375	0.0019	0.030	520	~200000
∅14	400	0.0020	0.025	540	~200000

3.3. Specimens

3.3.1. Specimen geometry

All the specimens have the same geometry. They are 1500 mm in height and 250x250 mm square in cross-section. Their cross-sections are increased at the top and bottom 400 mm region to 450x250 mm rectangular shape gradually. This was made to prevent a premature failure out of the test region. Fig. 3.5 shows the geometry of the test specimens.

3.3.2. Form work

Six specimens were cast vertically in two sets of three columns each by using steel forms. The steel form work was manufactured from 5 mm thick steel plates. Two channels facing each other were assembled in between two plates to form a single specimen unit. The form works consisted of three units connected each other with bolts. A base plate was also provided to ensure that the bottom ends of the columns were as flat as possible so as to ease the levelling of the specimens before testing. Details and dimensions of the form work are given in Fig.3.6.

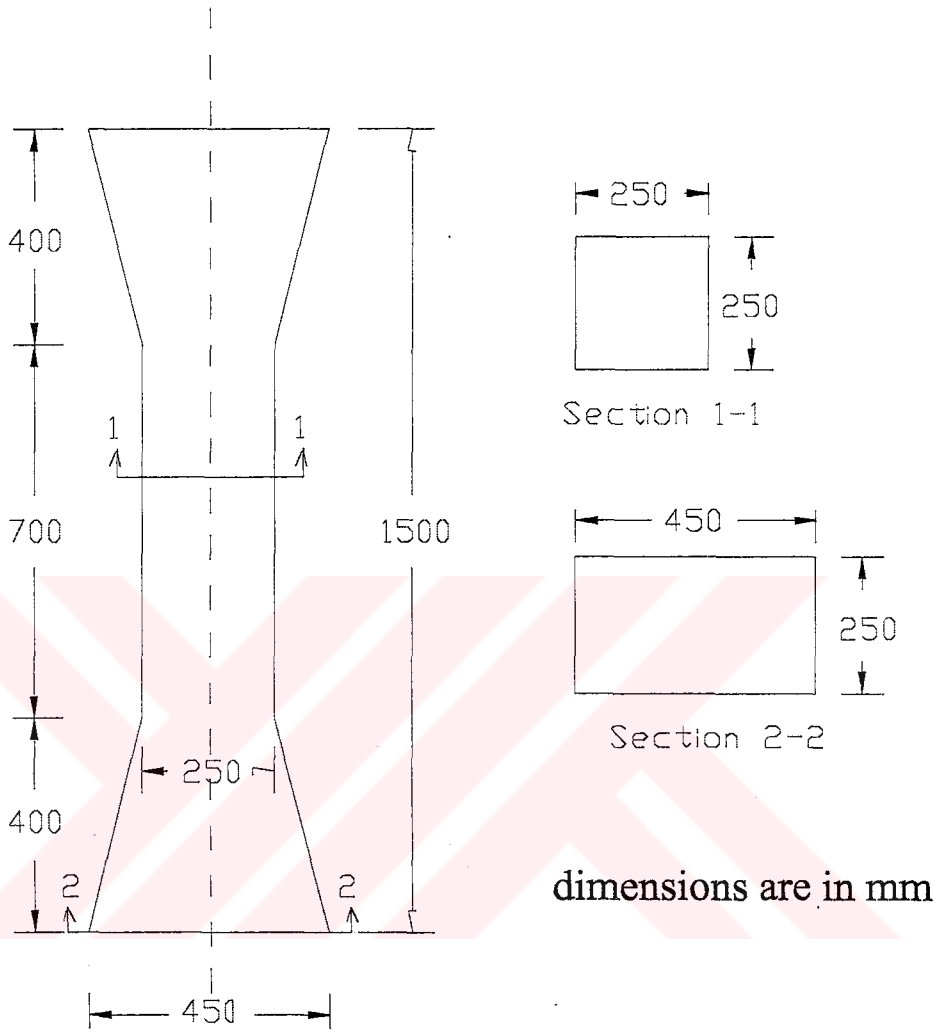

Figure 3.5 Geometry of the test specimens

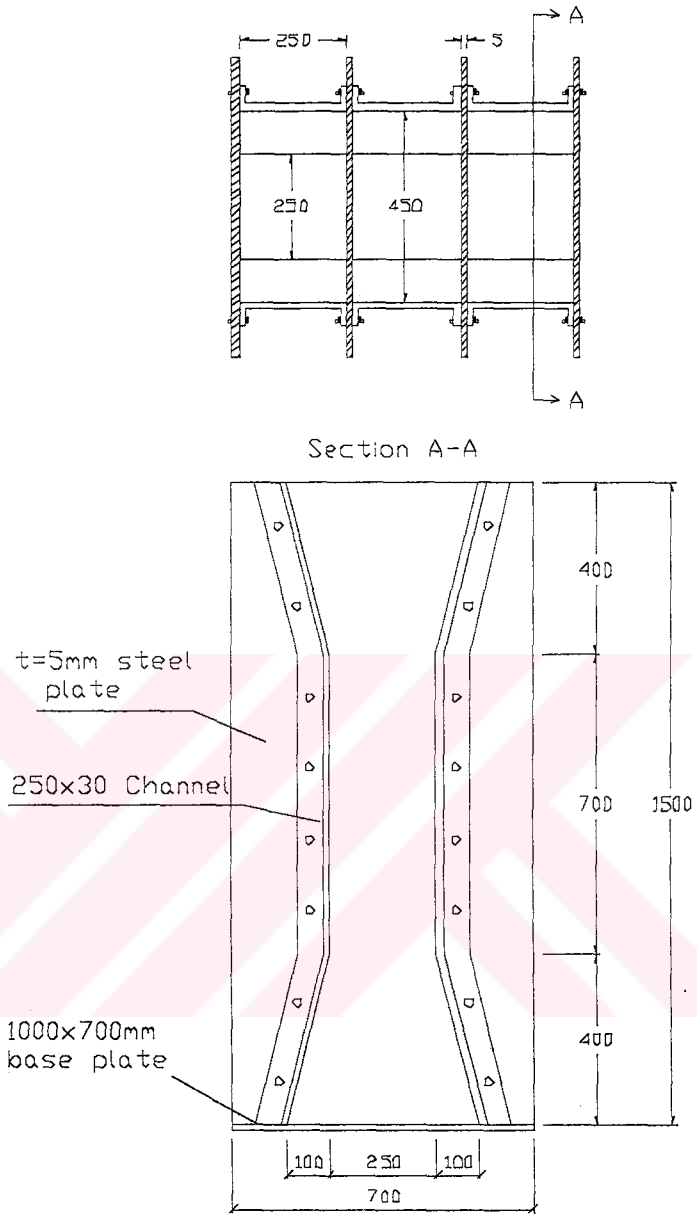

dimensions are in mm

Figure 3.6 Details of the Form work

3.3.3. Cages

All cages consisted of eight ∅14 longitudinal bars. Longitudinal bars were distributed uniformly over the perimeter of the cross section. Longitudinal bars were cut 15 mm shorter than the finished height of the specimens to ensure that they would not take direct load during the testing. In addition to the longitudinal bars, six ∅14 bars are provided at both ends of the specimens parallel to the inclination of the expanding section. At the ends of the specimens, tie spacing was also reduced nearly by half and heavy confinement is provided to force the failure to occur in the test region. Fig.3.7.a, b, c, and d show all the details of the specimens. In this figures configuration of the ties is also provided.

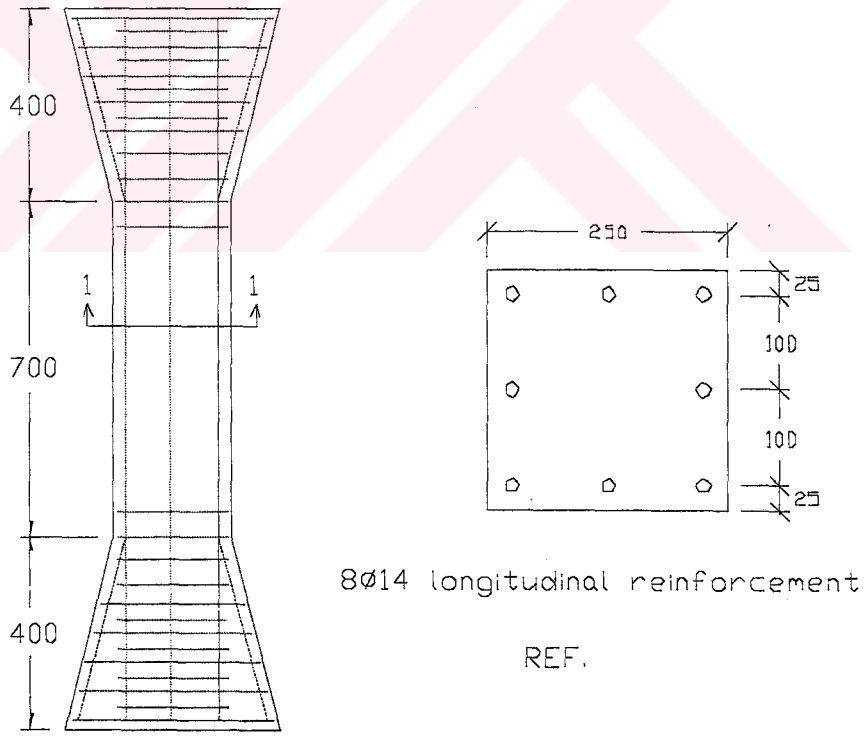

dimensions are in mm

Figure 3.7.a Details of the Reference Column

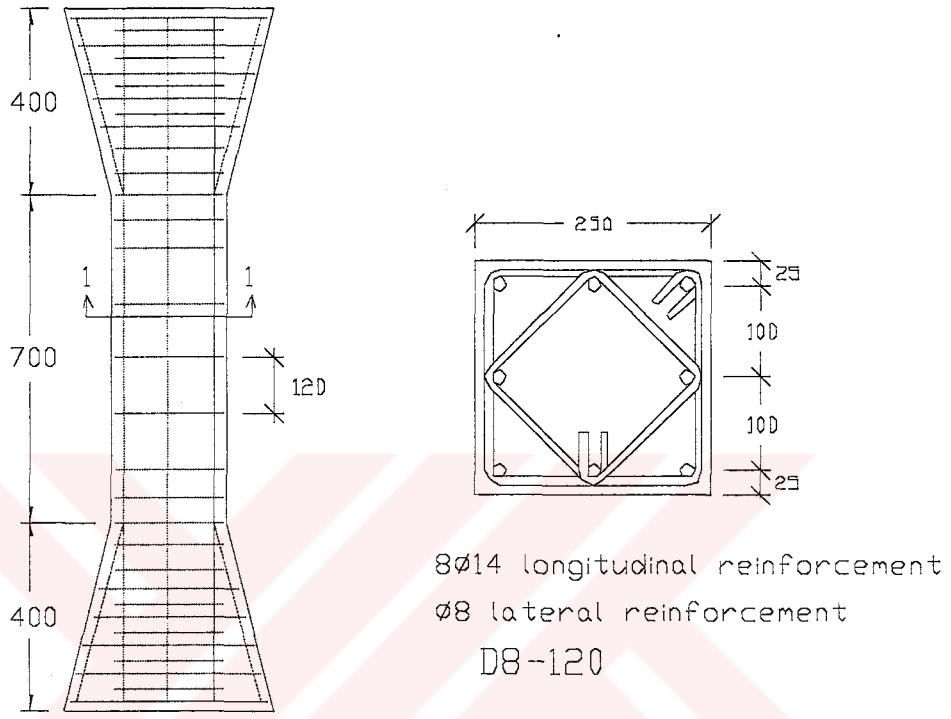

Figure 3.7.b Details of the Column D8-120

Table 3.3 shows the details of the confinement. In the second column of the table, the concrete cylinder strength, f_c, of the specimens at test day is given. In the last column of the table the mechanical ratio of transverse steel, $\rho_s f_{yt} / f_c$, is listed. This ratio is a good indication of the effectiveness of the confinement.

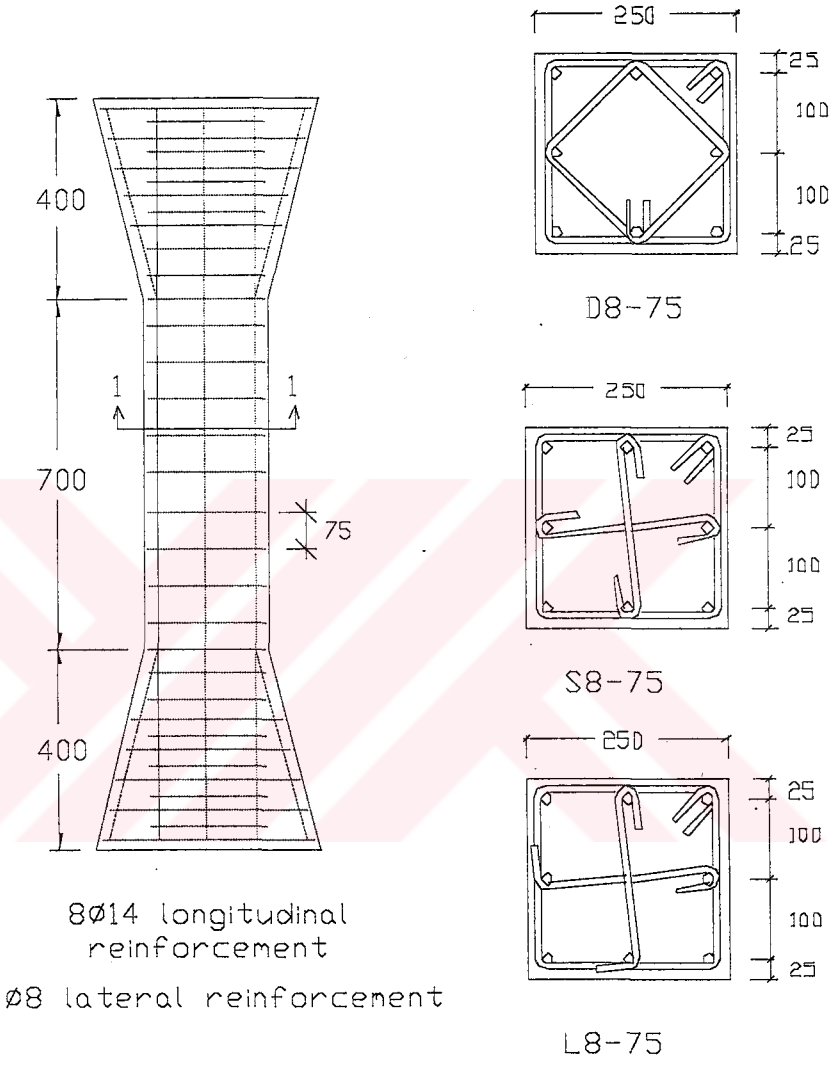

dimensions are in mm

Figure 3.7.c Details of Columns D8-75, S8-75 and L8-75

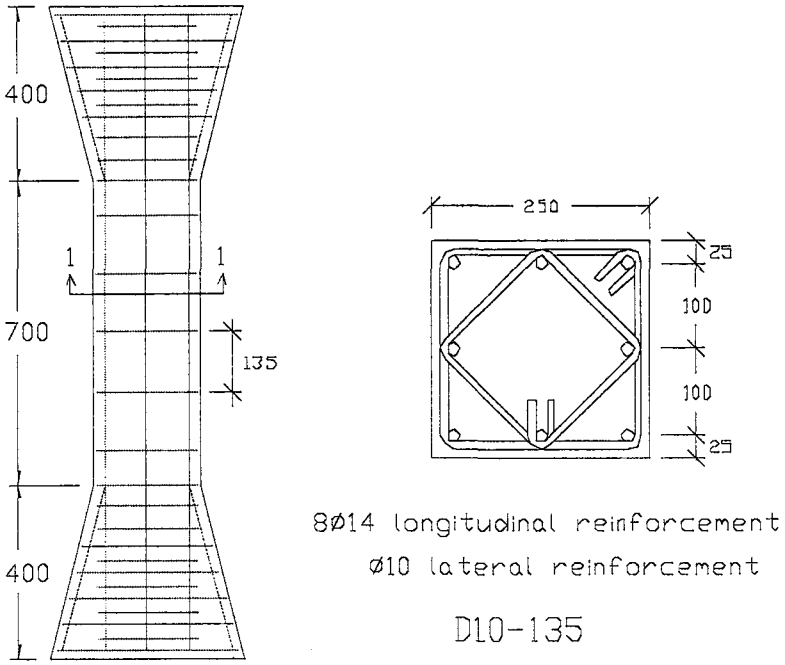

dimensions are in mm

Figure 3.7.d Detail of the column D10-135

Table 3.3 Details of the reinforcement

Column	f_c (MPa)	ρ (%)	f_y (MPa)	b_d (mm)	ρ_s (%)	s (mm)	f_{yt} (MPa)	$\rho_s f_{yt} / f_c$
REF.	85.0	1.97	400	---	---	---	---	---
D8-120	98.8	1.97	400	8	1.29	120	323	4.21
D8-75	89.5	1.97	400	8	2.06	75	323	7.44
D10-135	91.5	1.97	400	10	1.77	135	323	7.27
L8-75	91.5	1.97	400	8	1.81	75	323	6.39
S8-75	91.5	1.97	400	8	1.81	75	323	6.39

3.3.4. Casting and Curing

The column specimens were cast in two series using the concrete produced in the laboratory. The forms and control cylinder moulds were oiled before the placement of the steel cages in order to ease the stripping of the forms. Extra care was taken in order to keep the reinforcement oil free to assure a good concrete-to-steel bond. Concrete was placed in forms in about 3 to 4 layers. Each time columns were vibrated internally. In each casting, 15 control cylinders were also cast with columns. Concrete in cylinders was compacted by a poker vibrator externally.

All of the specimens were covered by wet burlap. Specimens and cylinders were stripped 3 days after casting. Following the stripping of the forms, specimens were wet cured by burlap cover. When the desired concrete strength was achieved, wet curing of the specimens were terminated and testing was performed in the following three days.

3.4. Instrumentation

3.4.1 General

In the instrumentation of the specimens Linear Variable Differential Transducers, LVDTs, and dial gauges were used for displacement measurements and load cell was used for load measurements. Load measurements were made by using a 5000 kN load cell. Deformations were measured by electronic dial gauges.

Voltage outputs from the instrumentation were fed into a data acquisition system. From there, all signals were directed to a personal computer. A software package written in the university stored the data as force and displacement. This program also monitored the data as numbers and graphics on the screen.

3.4.2. Deformation measurement

Deformations were measured vertically and horizontally on concrete in the test region of each specimen during testing. Kyowa-50A, Kyowa-20A and Kyowa-10A dial gauges were used to monitor the deformations taking place within the test region. The stroke capacities of these gauges were 50 mm, 20 mm and 10 mm respectively. Gauges were placed at the opposite faces of the bending direction. Vertical gauge length was 500 mm. Horizontal gauge length was 150 mm. Fig.3.8 shows the details of the instrumentation. For all specimens, the dial gauges were kept in position by steel rods embedded into the concrete core. The ends of the dial gauges were attached with piano wires to the steel rods. Shortening on the faces of the specimen was calculated from the average of the two dial gauge readings of that column.

Column deflection at midheight was measured by means of a LVDT. The data obtained from this LVDT were not meaningful. The reason for this might be the rigid body rotations and displacements of the specimens. To monitor this observation two more LVDTs were placed at the top and bottom of the specimens. Again the readings of these three LVDTs were not consistent. So it was concluded that the set-ups of the LVDTs were not correct. At column D8-120, another set-up was established. A thin wire was streched between the top and bottom ends of the column.

To read the deflection a horizontal scale was placed in the middle of the specimen as illustrated in Fig.3.8. During the test, the horizontal displacement readings were made by using a theodolite.

3.4.3. Load measurement

The column specimens were tested under eccentric axial load. Load measurements were taken with a 5000 kN capacity load cell. The load cell was calibrated before each test. During the test extra care was taken not to yield the load cell. Signals from the load cell were conditioned and amplified by the data acquisition system. The output signals were also transmitted to a computer where they were processed and stored on in force units.

3.5. Test set-up

The specimens were tested with a 5000 kN Losenhausen Hydraulic Test Frame which was located in the Materials Laboratory of Department of Civil Engineering. One rectangular 30 mm thick steel plate and one cylindrical 40 mm thick steel plate were placed both at the top and bottom of the column specimens. The load cell was placed under the bottom plate. The vertical alignment of specimens was done using thin layers of plaster at the top and bottom ends of the specimens to ensure the uniform distribution and to prevent stress concentrations during the application of the load on the specimen. Specimens were white washed to see clearly the cracks occurring during the test. Fig.3.8 shows the instrumentation and the test set-up.

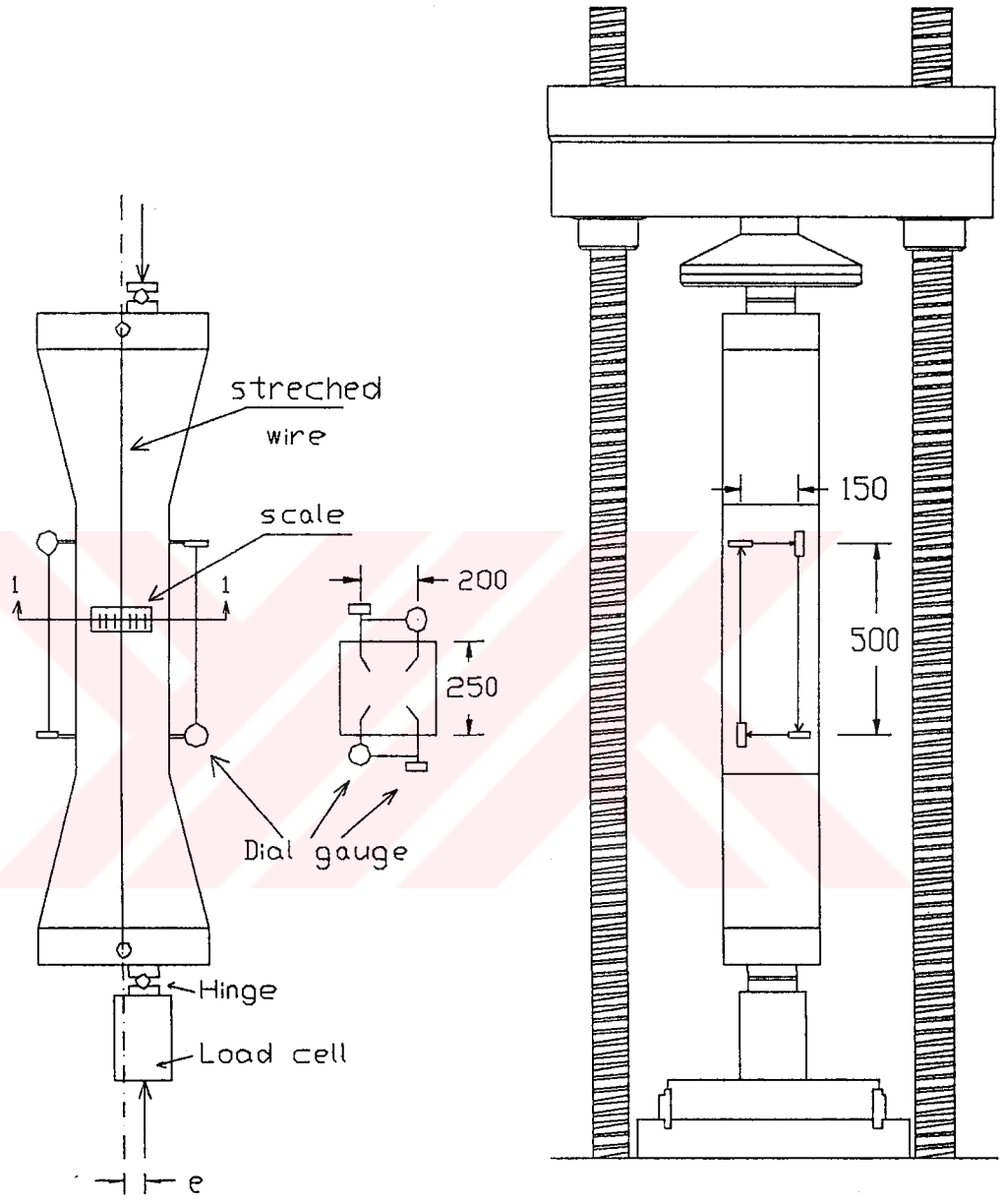

Figure 3.8 The instrumentation and the test set-up

3.6. Test procedure

To ensure required eccentricity extra care was taken for vertical alignment of the specimens. Test machine was load controlled. Therefore, descending part of the stress-strain curve could not be recorded because of the limitations resulting from the test machine. Failure was brittle and instantaneous for all specimens. Right after the test, three cylinders were also tested to determine the strength of the concrete.

CHAPTER IV

OBSERVED BEHAVIOR OF TEST SPECIMENS

4.1 General

In this chapter the observed behavior of the test specimens will be presented. For all the specimens longitudinal and lateral displacements were read simultaneously by the applied load. From these data Load vs. Strain curves were drawn.

All the six specimens were tested under same conditions. For all specimens only one type of loading was used: eccentrically applied axial load. The formation of the moment was ensured with eccentricity, that is the load was applied with 20 mm offset measured from the center-line. Eccentricity was limited by this 20 mm to ensure to keep the load in the kern of the section, so that no tension would develop in the cross-section. The limits of the kern and the point of application of the load are shown in Fig.4.1.

Strains for the curves were calculated by dividing the average of the two dial gauge readings to the gauge length. The load data stored in the computer were in force units. Therefore, they were not processed.

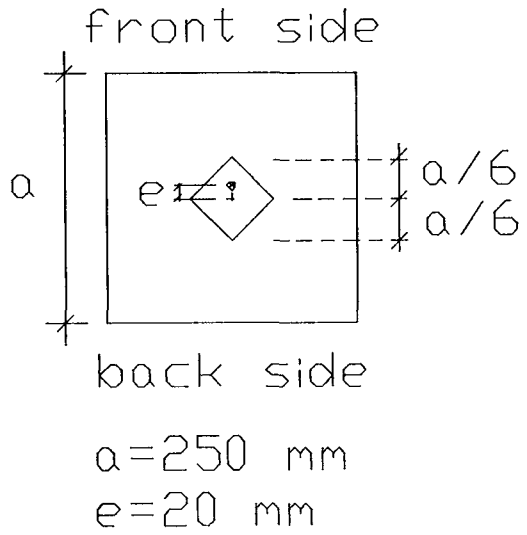

Figure 4.1 Application point of the load and limits of the kern

4.2 Observed Behavior of the Specimens

In this section load versus average strains were presented for each specimen. The test was load controlled; therefore, the accuracy in descending part of the curves were restricted with the data reading speed of the data acquisition system. The failure for all specimens was brittle and instantaneous. Therefore, the descending branch could not be obtained.

4.2.1 Reference Specimen

The reference specimen had no confining reinforcement at the test region. This specimen was tested to understand better the behavior of confined column tests. The reference column was loaded with an eccentricity of 20 mm. The failure occured

at 3890 kN. The peak strain in the front longitudinal direction was 0.0024. The front lateral and longitudinal strains vs. load are shown in Fig.4.2. The curve was almost linear until high load levels, approximately 80% of the maximum load. The specimen displayed a very brittle response and the failure was explosive . The cylinder strength of concrete was 85 MPa on the test day.

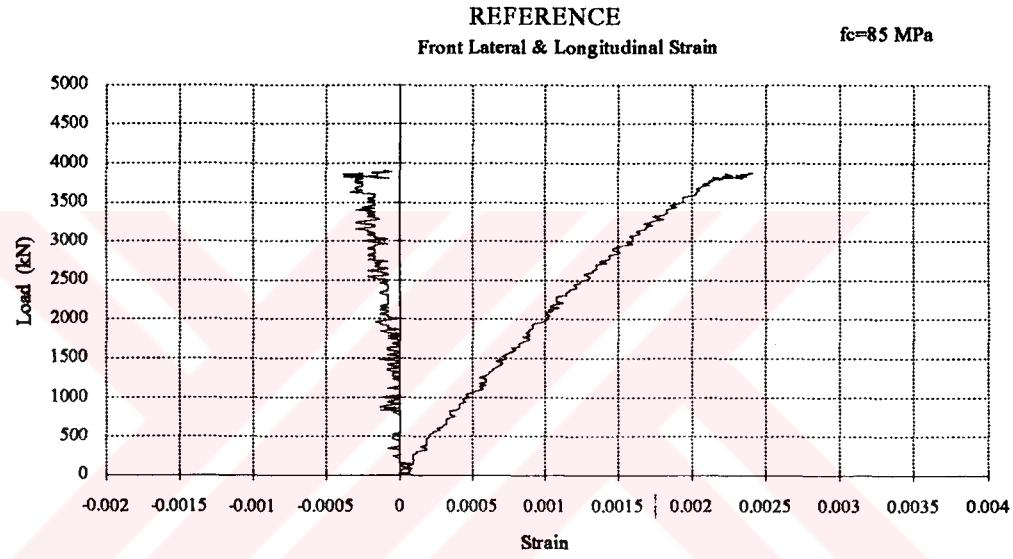

Figure 4.2 Lateral and longitudinal front strains of the specimen Reference

Fig.4.3 shows the average back strains of the reference specimen. The lateral back strain is almost zero and the longitudinal back strain is one fourth of the longitudinal front strain.

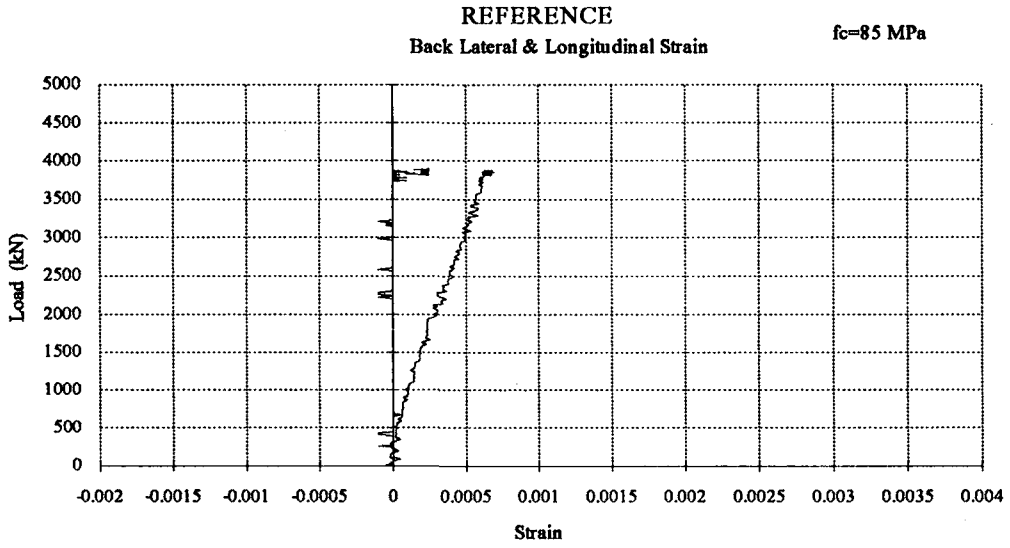

Figure 4.3 Lateral and longitudinal back strains of the specimen Reference

4.2.2 Specimen D8-120

Specimen D8-120 had 8 mm ties with a tie spacing of 120 mm in the test region. This specimen had a volumetric ratio ρ_s of 1.29 and a mechanical ratio (or reinforcement index), $\rho_s f_{yt} / f_c$, of 4.21. This ratio is a good indication of the effectiveness of the confinement.

At the beginning of the test, the aim was to load the specimens concentrically. At the first two attempts on specimen D8-120, the load was axially concentric. At the first test, the load was increased until 4860 kN. Neverthless the data saved in the computer were only upto 4540 kN, because the gain of the data acquisition system for the load cell channel was higher than the limits of the system. Therefore, the load was removed and the gain was so calibrated that it will be kept

within the limits. On the same day the second loading of the specimen D8-120 was performed by the correct set-up of the data acquisition system. At this attempt, the specimen was loaded and unloaded three times. The failure did not occur. At these two loadings, the cylinder strength of concrete was 82 MPa. Next day, the test was repeated with 20 mm eccentricty. This time, the head of the specimen failed prematurely at 3100 kN. The reason was the inadequate thickness of the rectangular steel plate. It could not spread the load evenly. Stress concentration occured due to plate deformation and therefore failure took place just under the application point of the load. To prevent this kind of failure additional circular 40 mm thick plates were provided at both ends of the specimens. Concrete at cracked region of the head was removed and the buckled bars were strengthened with additional steel bars in the tapered end zone. Additionally, steel jacketing was made with 5 mm thick plates to prevent the repetition of the premature failure. These welded plates served also as form for concrete. The same high strength concrete was prepared and molded in the steel form. The form was kept in wet burlap until the required concrete strength was reached.

At the fourth loading of specimen D8-120, the column was loaded with 20 mm eccentricty two times until 4860 kN; but failure did not occur. The concrete had gained very high strength, because of the time delay caused by the complications explained above. On the test day the cylinder strength of the concrete reached up to 97 MPa. At the last attempt the eccentricity was increased up to 30 mm. This time the column failed at 4610 kN in a brittle manner.

The longitudinal back strains are almost zero for all tests. Therefore, the curves for the back face of the columns were not presented. Fig.4.4 shows the lateral

and longitudinal strains of the front side of the specimens. The curve shows that with the repetition of the load, stiffness of the column decreases. The descending part of the curve could not be recorded because failure was brittle and instantaneous. The failure occurred approximately at 0.004 strain and 4600 kN load.

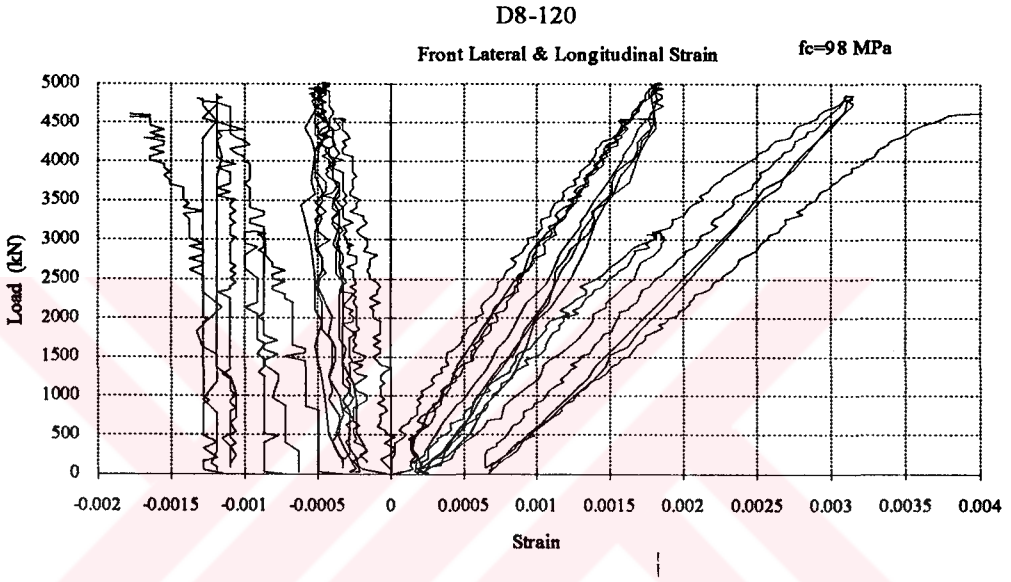

Figure 4.4 Lateral and longitudinal front strains of the specimen D8-120

Fig.4.5 shows the back strains of the specimens. In this curve first two tests were not drawn, because these two attempts were concentrically axial load tests. Therefore, back strains are almost the same with the front strains.

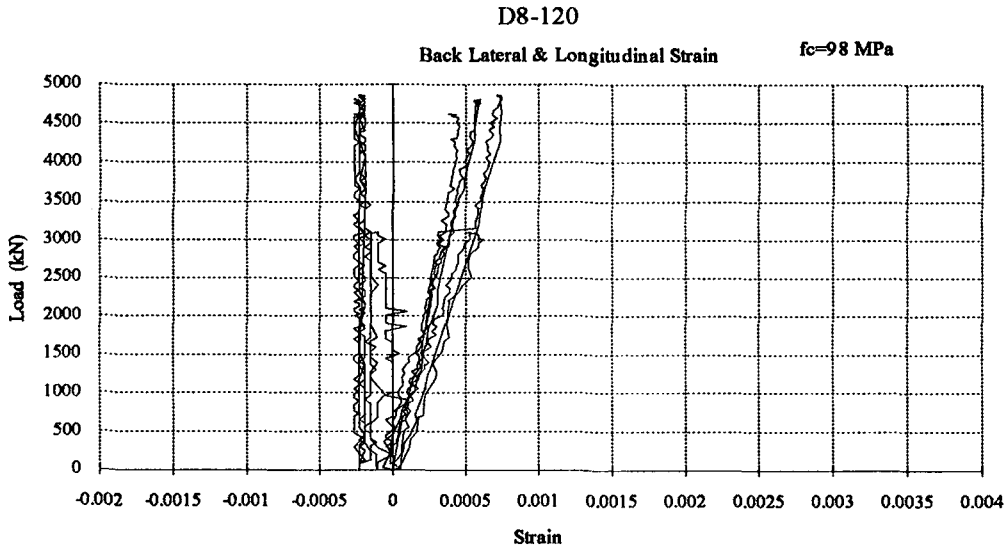

Figure 4.5 Lateral and longitudinal back strains of the specimen D8-120

4.2.3 Specimen D10-135

Specimen D10-135 had 10 mm lateral bars and 135 mm tie spacing in the test region. Specimens D10-135 and D8-75 are two comparison specimens having equal $\rho_w f_{yw}$ values. The mechanical ratio of this column was 7.27.

The test was completed without any problem. The failure of the column occurred at the first loading. Fig.4.6 shows the lateral and longitudinal front strains. In this test, cover crushing began at 4150 kN and failure occured at 4240 kN. The peak strain was approximately 0.003. The back strains are shown in Fig.4.7. The proportion of the longitudinal front to the longitudinal back strain is approximately seven. The cylinder strength on the day of testing was 91.5 MPa.

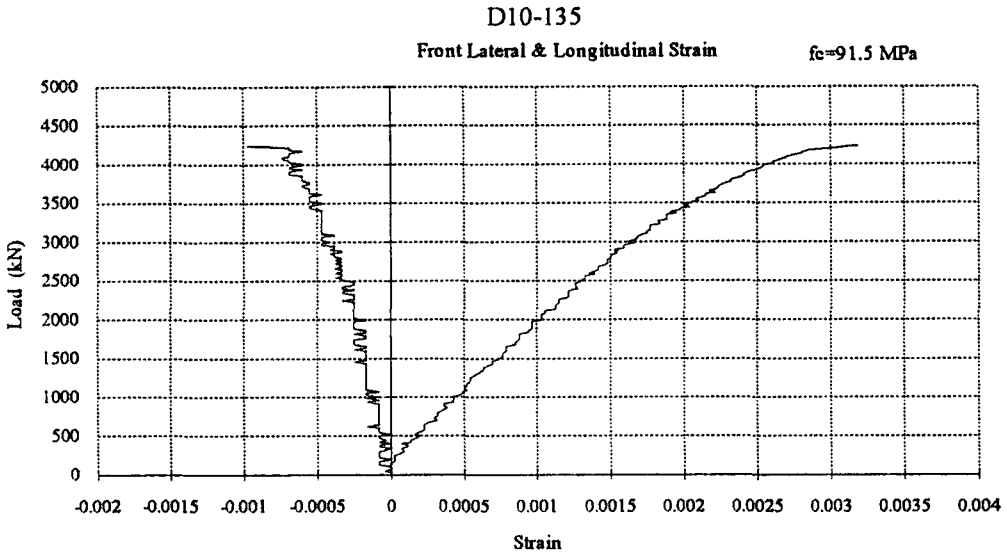

Figure 4.6 Lateral and longitudinal front strains of the specimen D10-135

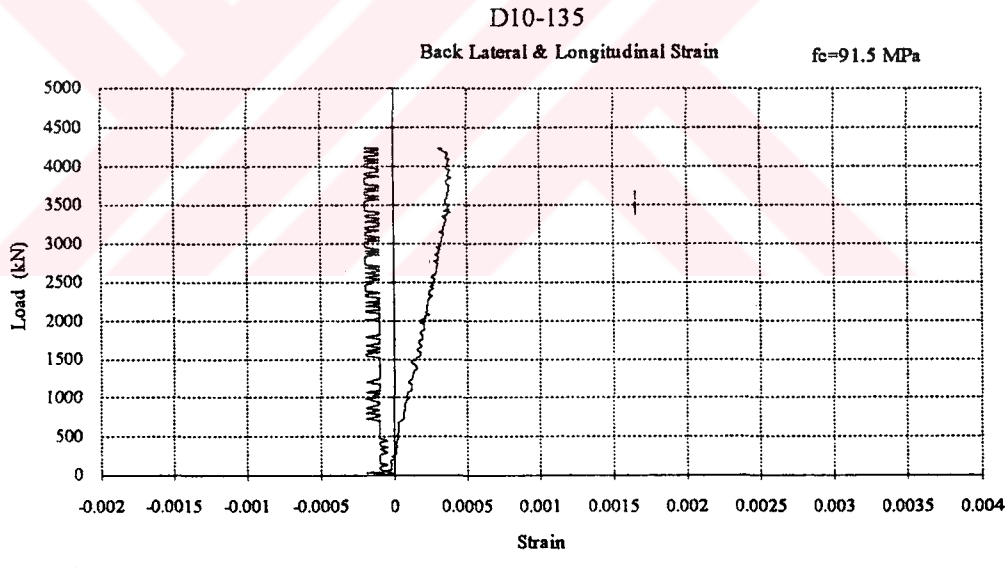

Figure 4.7 Lateral and longitudinal back strains of the specimen D10-135

4.2.4 Specimen L8-75

Specimen L8-75 was designed to study the effects of cross ties. It would be compared with S8-75 for their cross-tie efficiency. Specimen L8-75 had a standard hook with bend of 135° at one end and a standard hook with a bend of 90° at the other end. On the other hand, specimen S8-75 had a standard hook with bend of 135° at both ends. Specimen L8-75 would also be compared with D8-75 for the tie configuration efficiency.

This column had lateral bars of 8 mm in diameter and a tie spacing of 75 mm. It was assumed that the L-ended cross-ties will not make its function properly. Therefore, the cross-tie was ignored in the calculations of the volumetric ratio of transverse steel and mechanical ratio of the column. This specimen had a mechanical ratio of 4.26. The load vs. strain curve, Fig.4.8, showed that it works as efficient as specimen S8-75. The peak load for this column was 4600 kN. The peak strain was 0.0031. Fig.4.9 shows the lateral and longitudinal back strains. The longitudinal back strain was one sixth of the longitudinal front strain. The concrete cylinder strength of the column was 91.5 MPa.

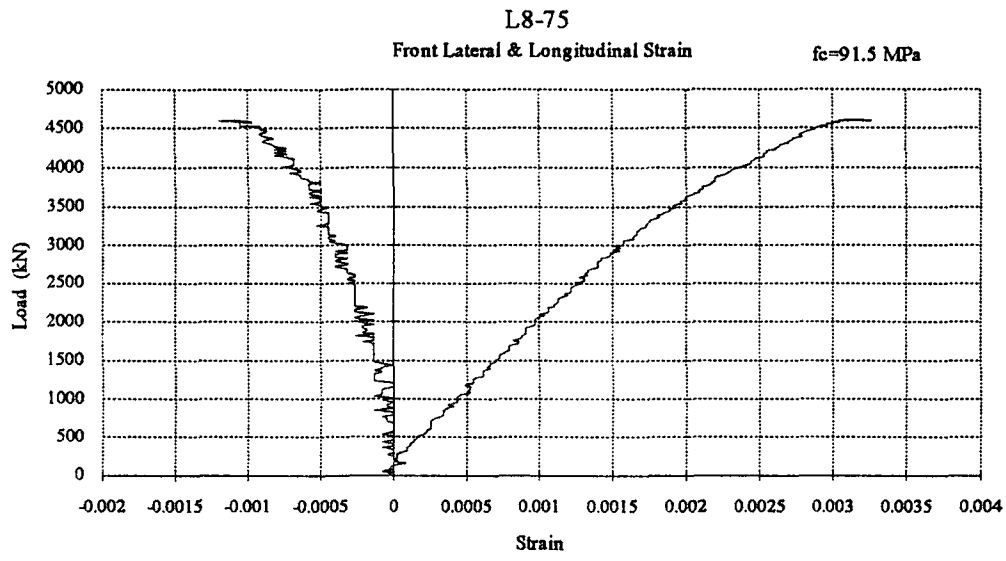

Figure 4.8 Lateral and longitudinal front strains of the specimen L8-75

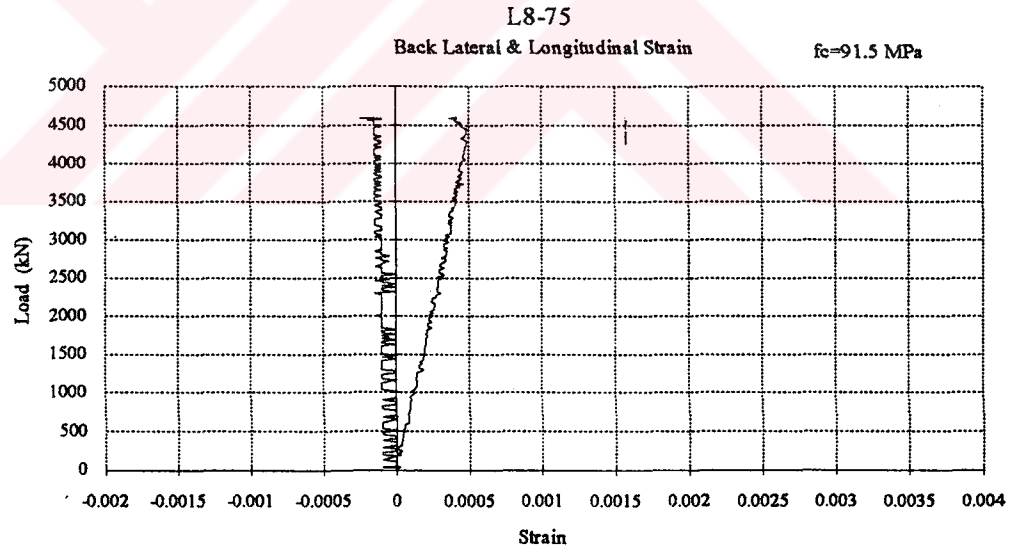

Figure 4.9 Lateral and longitudinal back strains of the specimen L8-75

4.2.5 Specimen S8-75

Specimen S8-75 had also cross-ties confining the facing midside bars. The lateral confinement has the diameter of 8 mm and the tie spacing 75 mm in the test region. The cross-ties had a standard hook with bend of 135° at both ends. Cross-ties are used widely in constructions. Therefore, the usage of the cross-ties with high strength concrete should be studied.

Fig.4.10 and Fig.4.11 show the front and back strains respectively. The column was failed at 4460 kN. The peak strain of this column was 0.0034. The longitudinal front strain curve was almost linear up to 70 % of the peak load. The concrete cylinder strength of the specimen was 91.5 MPa.

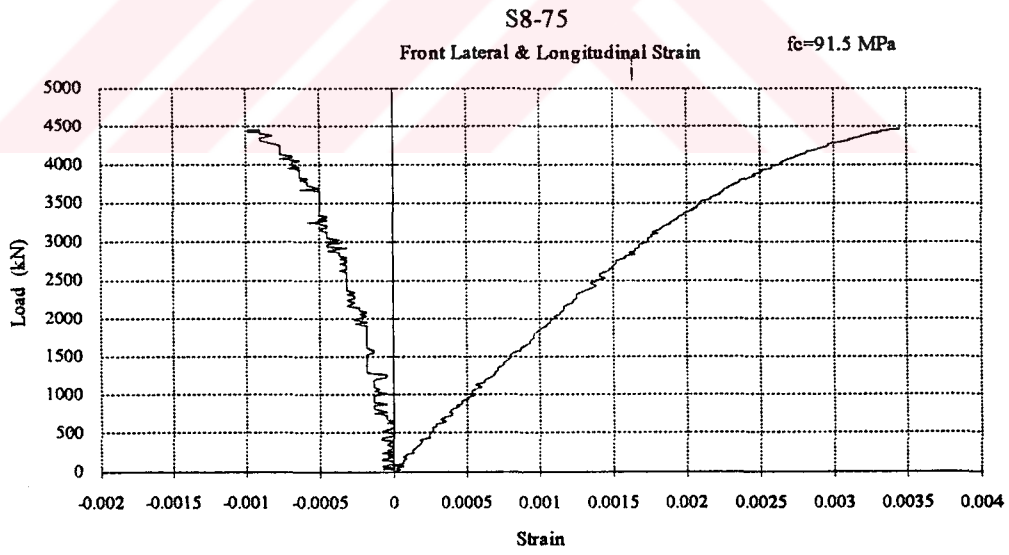

Figure 4.10 Lateral and longitudinal front strains of the specimen S8-75

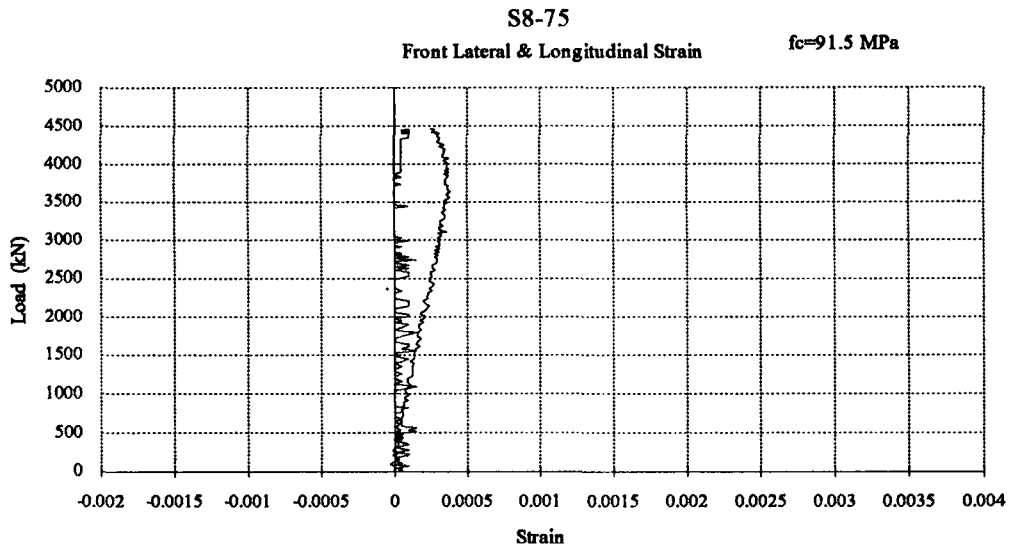

Figure 4.11 Lateral and longitudinal back strains of the specimen S8-75

4.2.6 Specimen D8-75

Specimen D8-75 had 8 mm in diameter lateral steel bars with a tie spacing of 75 mm in the test region. This specimen had the highest volumetric ratio ρ_s with a value of 2.06 and its mechanical ratio $\rho_s f_{yt} / f_c$ was also the highest one which was equal to 7.44.

At the first loading of the specimen D8-75, load was removed from the column at 3220 kN, because the dial gauge readings showed biaxial bending. Necessary adjusments were made and the alignment of the column was controlled very carefully. Load cell gave unreasonable readings at the second loading of the specimen. Therefore the test was interrupted and load cell was controlled. The reason

of the unexpected load cell behaviour could not be found. The load cell was recalibrated. Because of the incorrect data acquisition of the load, the curve could not be drawn; but the displacement readings were correct. Therefore, strains were calculated. In Fig.4.12 and Fig.4.13, only the first and third curves are presented. Failure was reached in the third loading. At a load stage of 3970 kN cover crushing began and at 4619 kN the column failed. The failure of this column was also brittle. The longitudinal front strain at failure was 0.0032. Although, this column had the highest mechanical ratio, even this confining reinforcement was inadequate for a ductile behavior.

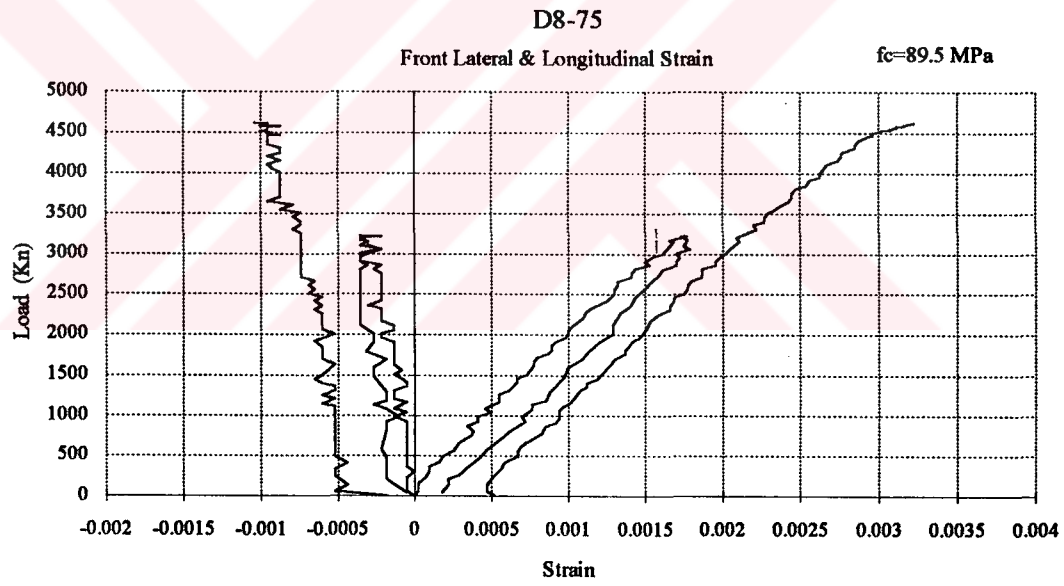

Figure 4.12 Lateral and longitudinal front strains of the specimen D8-75

On the test day of the column D8-75, the cylinder strength of concrete was 89.5 MPa. Fig.4.13 shows the lateral and longitudinal back strains. The ratio of the longitudinal front strain to the longitudinal back strain was approximately six.

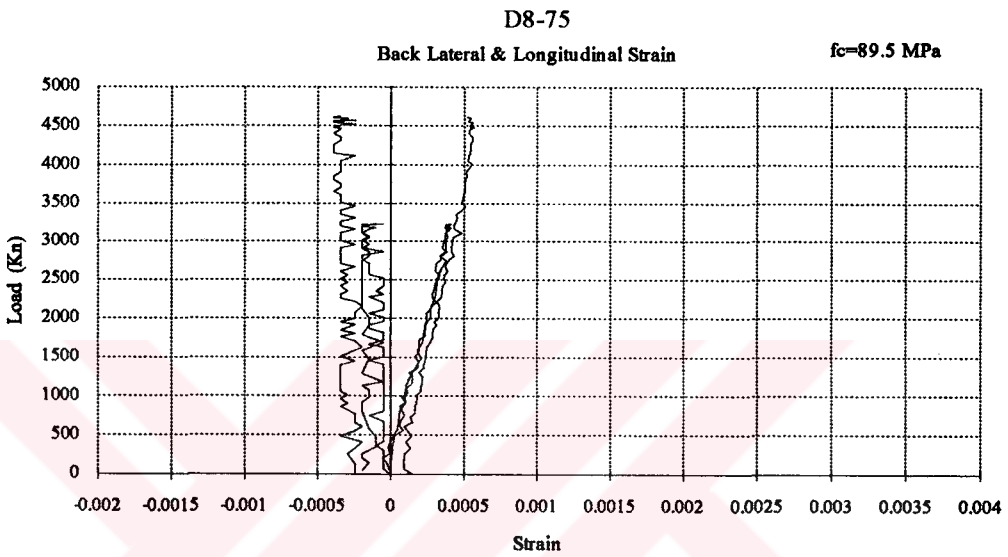

Figure 4.13 Lateral and longitudinal back strains of the specimen D8-75

CHAPTER V

ANALYSIS AND DISCUSSION OF TEST RESULTS

5.1 General

In this chapter, the test results were analysed and compared with the analytical results. Experimentally obtained stress-strain curves were compared with the concrete models. The models, used in the analytical studies, were Nielsen, Sheikh&Uzumeri and Nagashima models. These models are described in Appendix A. Sheikh&Uzumeri model was chosen because it was a widely used model that satisfactorly represents the behavior of NSC and it was also modified for HSC. Nielsen model was selected due to its simplicity. It had a triangular shape. This model was drived for plain HSC; but it was used for confined concrete with a modification in this study. Nagashima model was developed for HSC and UHSC with high or ultra-high strength reinforcing bars.

The moment-curvature curves were drawn for each specimen. The normal force-moment pairs corresponding to ultimate limit state were finally marked on the interaction diagram drawn for each specimen. The graphs showing the load vs. poisson's ratio were drawn to study the variation of the Poisson's ratio.

Computer programmes were utilized in order to apply the concrete models to the test results. These programmes were purpose oriented; for this reason they were problem dependent and not user-friendly. Therefore, the source codes of these programmes were not included in this thesis. Reduced experimental data and the analysis results were plotted by means of the computer programme MS-Excel 4.0.

5.2 Comparison of the load-strain curves

The comparison of the load-strain curves were made in term of the applied axial load vs. average front strain diagrams. In this study average back strains were not included. They were nearly zero, therefore insignificant. For evaluating the analytical models a computer programme was developed. The procedure of the programme was as follows:

1. chose a top strain
2. chose a neutral axis depth, c
3. calculate the normal force N and the moment M
4. if M/N is not equal to the required eccentricity then change the neutral axis depth and go to step 2. Repeat these steps, "iteration", until the equilibrium is satisfied.
5. if M/N is equal to the eccentricity of the test, then this should be the searched point; calculate also the curvature and the bottom strain.
6. increase the top strain and go to step 2. Repeat these steps until the top strain reaches its maximum value.

The load-strain curves obtained according to the above procedure were presented inFig.5.1 to Fig.5.6. All analytical models used in this study predicted the load carrying capacity of the specimens satisfactorily. The ascending part of the load-strain curves obtained from the Nagashima and Nielsen models agreed quite satisfactorily with the experimental ones. For HSC the ascending part of the load-strain curve is almost linear, whereas the analytical diagram of the Sheikh&Uzumeri model shows a curved initial part. For this reason, in all experiments the load was overestimated by 20-35% when Sheikh&Uzumeri model is used. The Nagashima concrete model provides the best prediction among the three analytical models used in this study.

The curves related to reference Specimen were shown in Fig.5.1. For this specimen all models yielded satisfactory predictions of the experimentally observed response. Nagashima curve somewhat overestimates the maximum strain by 25 %. The peak load and strain for this specimen were 3900 kN and 0.0022 respectively.

In Fig 5.2 the first two loadings of specimen D8-120 are not drawn, because the load was applied concentrically in this test. Maximum difference between the experimental load and analytical load calculated by Sheikh&Uzumeri model was 35% in this experiment. Nielsen curve drops sharply after the peak since the model itself, has a very steep descending part in its original form. This is reasonable because Nielsen model is an unconfined concrete model. Specimen D8-120 carried 4620 kN load.

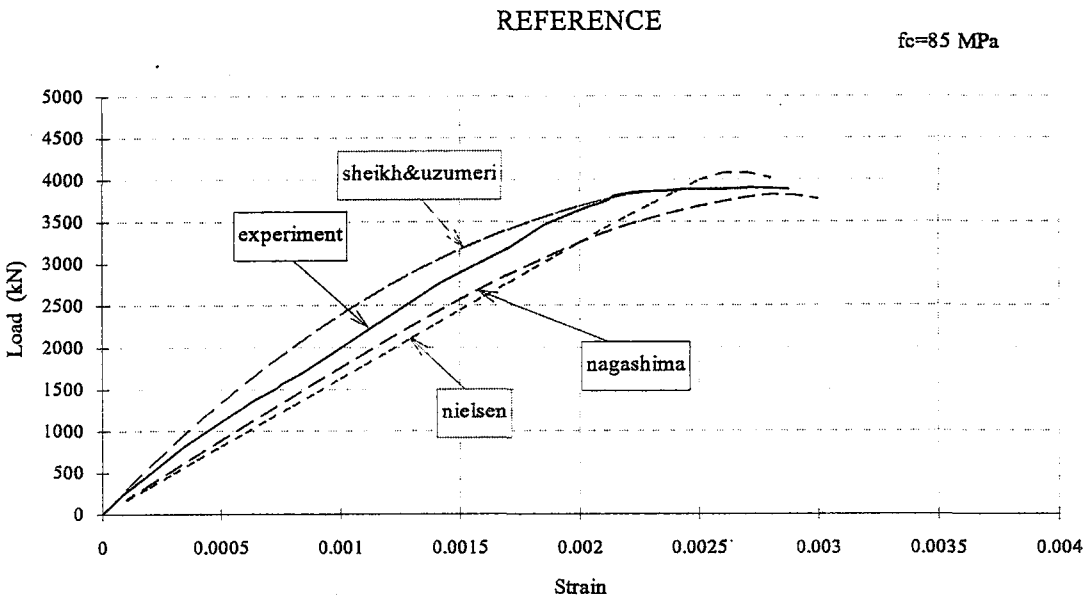

Figure 5.1 Load vs. front average strain of specimen Reference

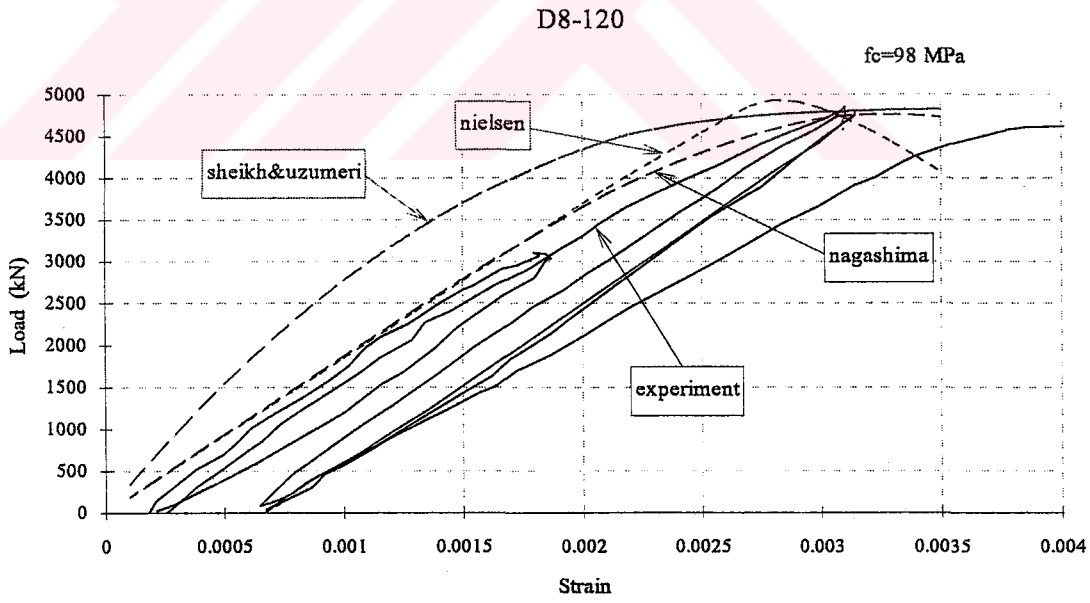

Figure 5.2 Load vs. front average strain of specimen D8-120

All the three models nearly overestimated the experimental peak load of specimen D10-135 (Fig.5.3). This might be due to large tie spacing that does not enable the concrete gain the calculated strength. Neverthless, the variation is within the experimental scatter. The difference was approximately 9% for the peak load. The peak load for specimen D10-135 was 4240 kN. The strain at the peak was approximately 0.003.

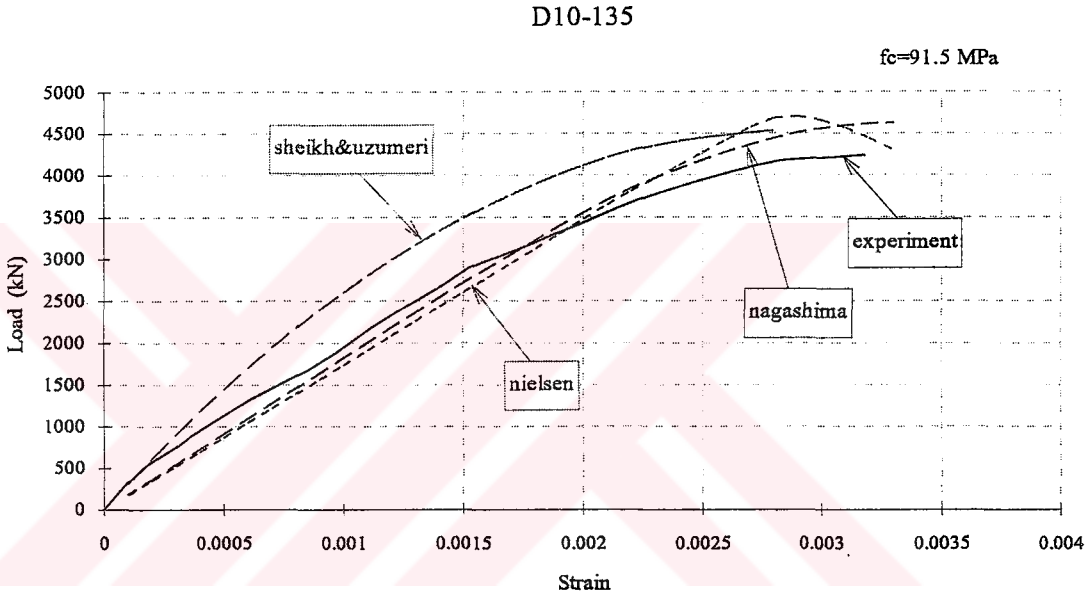

Figure 5.3 Load vs. front average strain of specimen D10-135

Comparisons made for L8-75 and S8-75 produced similar results (Fig.5.4 and Fig.5.5): For all cases the experimental load vs. front average strains were predicted better by the Nagashima curve among the three analytical models used in this study. Load carrying capacity for specimen L8-75 and S8-75 were 4600 kN and 4460 kN respectively. The strain at their peak were 0.0031 and 0.0034 respectively.

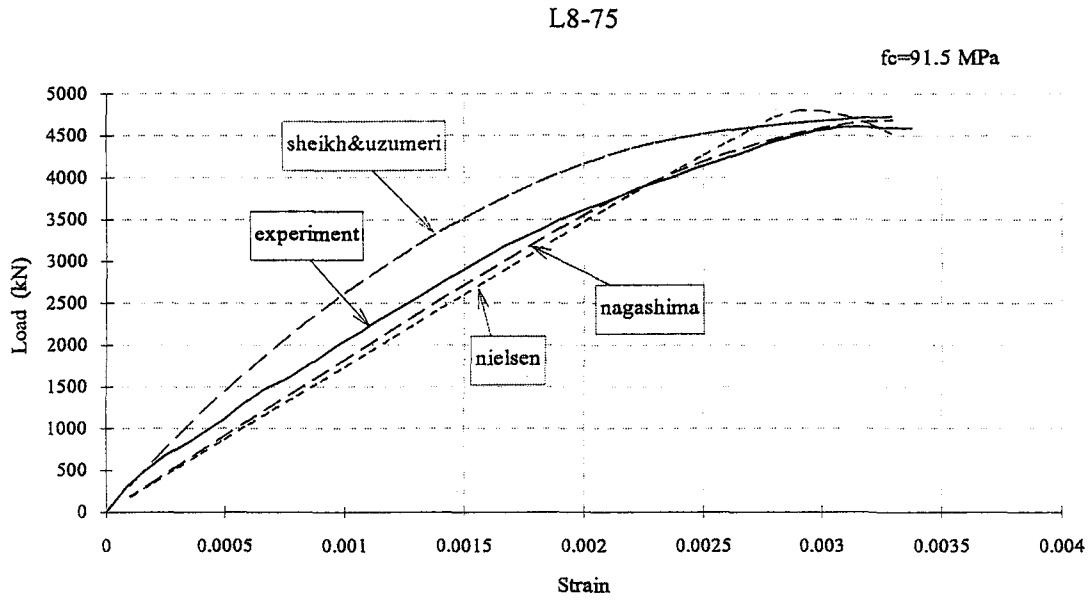

Figure 5.4 Load vs. front average strain of specimen L8-75

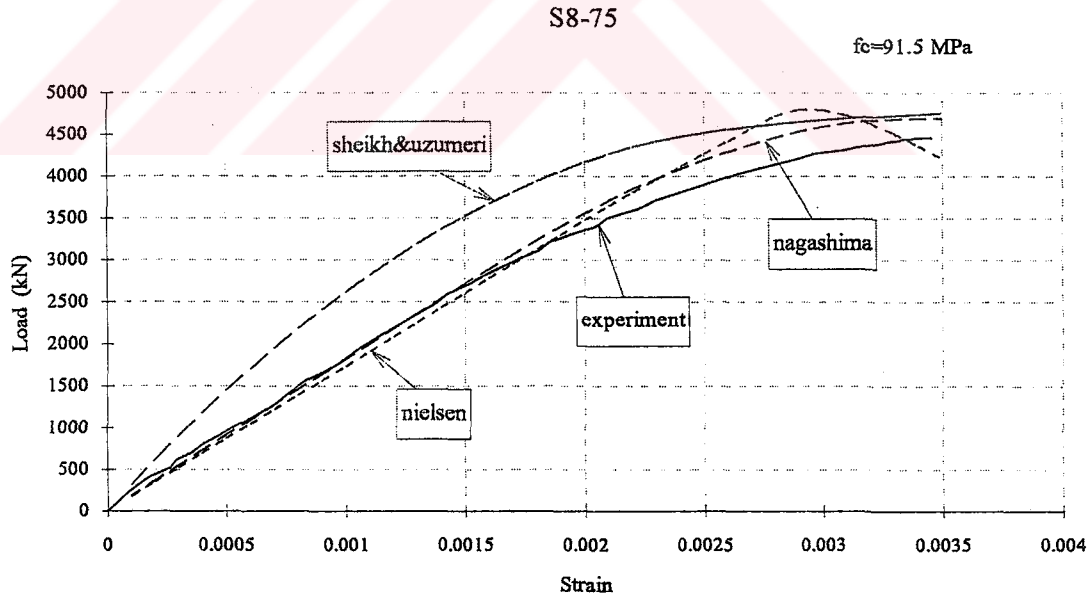

Figure 5.5 Load vs. front average strain of specimen S8-75

Specimen D8-75 has the highest confinement ratio. This column failed in a brittle manner. The provided confinement prevented only the explosive type of failure that has been observed at reference Specimen. Fig.5.6 shows that the best matching to the experimental curve is assured by Nagashima curve. The peak load of the specimen was 4620 kN and the peak strain was 0.0032.

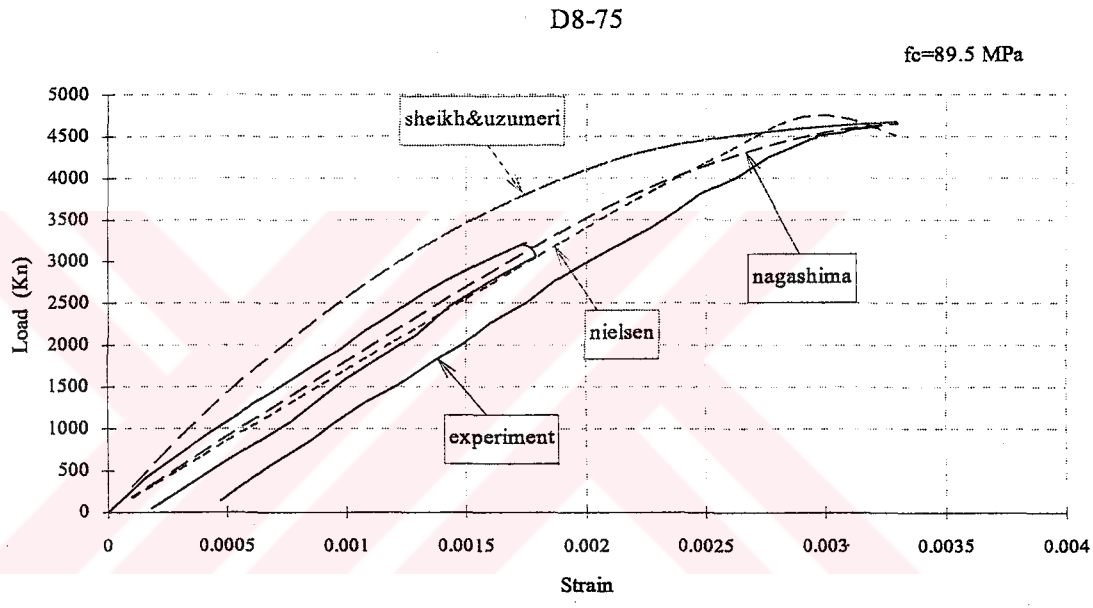

Figure 5.6 Load vs. front average strain of specimen D8-75

5.3 Comparison of the moment-curvature curves

In this section, the experimental moment-curvature curves were compared with the theoretical curves drawn according to the three analytical concrete models. Analytical moment-curvature (M-φ) values were produced as a by-product of the

load-strain calculations in section 5.2. To calculate the experimental curvature, first, the two longitudinal strains at both faces of the column were averaged. Curvature was found by dividing the average strains by the distance between them. First order experimental moments were computed by multiplying the applied axial load by the eccentricity. Three horizontal LVDTs mounted at the top, bottom and the mid-height of the specimen to calculate the moment generated from p-Δ effect. This set-up did not work. Therefore, another set-up explained in section 3.4.2 was established with piano wire, scale and theodolite. This set-up was used in specimen D8-120 loaded at 30 mm eccentricity. The readings showed that there was approximately 10% increase in eccentricity due to second order effects. It was concluded that the second order moment, ΔM, of 20 mm eccentrically loaded specimens should be less or equal to 10% .

In this section, two moment-curvature diagrams are given; (a) based on first order moments, (b) based on total moment including the second order effects. Moment-curvature diagrams obtained from the analytical models were expected to lie between the two experimental curves. The dispersion of the analytical curves from the limits may be due to:

- a possible weakness (weak plane) of the element
- a possible shift in the eccentricity during the experiment
- reliability of the analytical models

Nevertheless, the variation is within the experimental scatter; 10-15% difference for concrete may be concidered acceptable.

The moment-curvature diagrams were shown from Fig.5.7 to Fig.5.13. Moments in this graphs were given in kN-m and curvatures in rad/m. For all figures Nagashima curve among the three models showed the best matching with the experimental response. Analytical curves obtained from Sheikh&Uzumeri model somewhat overestimated the experimental moment in the ascending part. Nielsen curve showed always an early drop, however it predicted initial slope quite satisfactorily.

The moment-curvature diagrams of the reference specimen are shown in Fig.5.7. Agreement between the experimental and analytical values were quite satisfactorly.

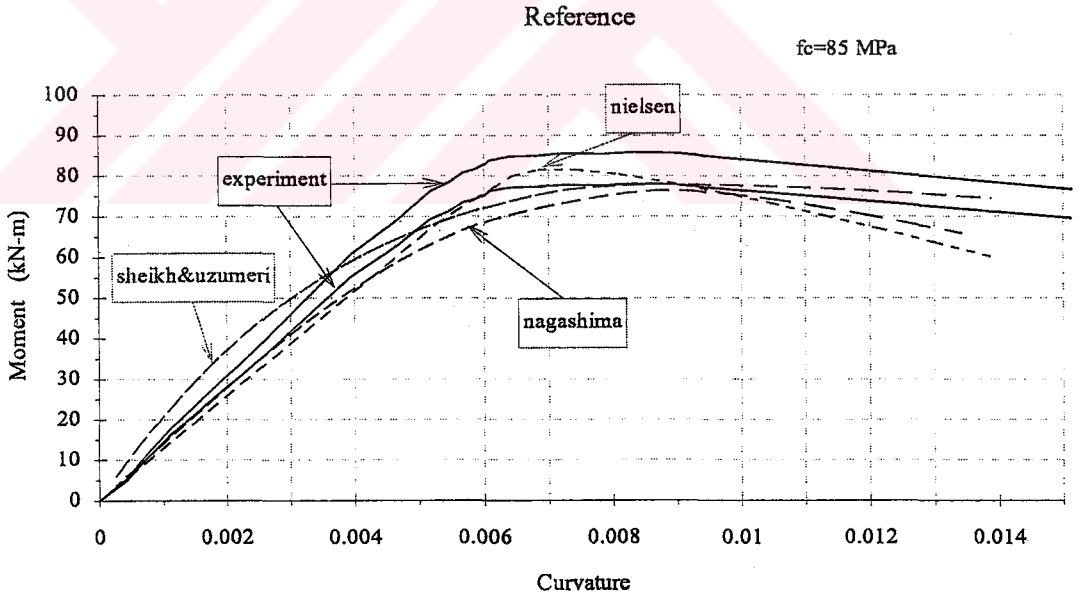

Figure 5.7 Comparison of moment-curvature curve of refernce specimen

The moment-curvature relation of specimen D8-120 was presented on Fig.5.8 and Fig.5.9. This specimen was loaded five times. The first two loadings were axial concentric. Therefore, they were not be included in the figures. Fig.5.8 shows the third and fourth loading, where the eccentricity was 20 mm. The second order curve was not plotted on the diagram, because the column was loaded several times. The last loading with 30 mm eccentricity was shown in Fig.5.9. In this figure all the analytically obtained curves underestimated the peak moment by about 7%.

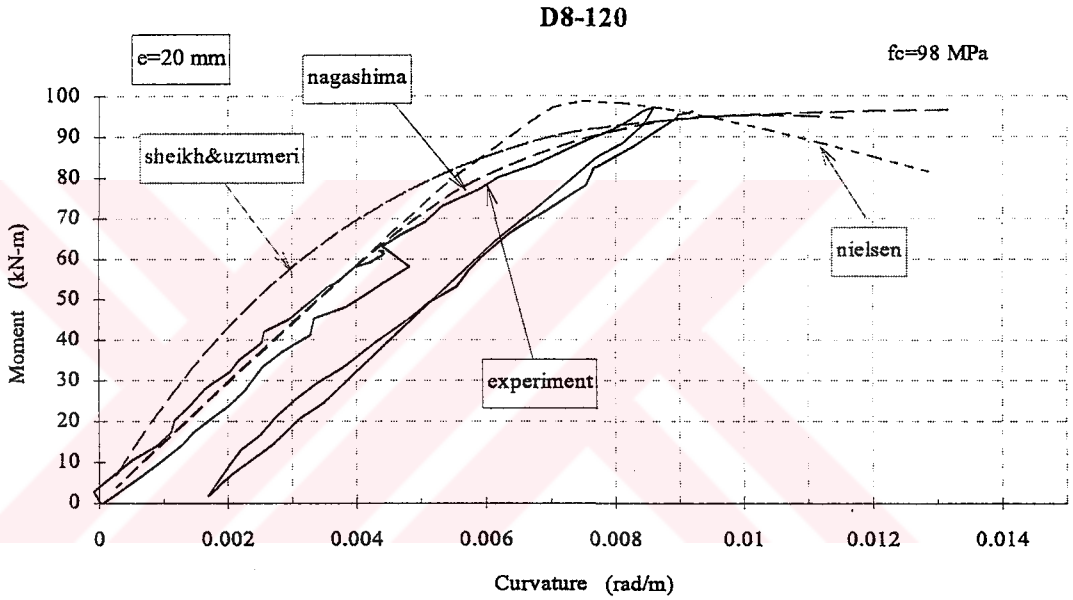

Figure 5.8 Comparison of moment-curvature curve of specimen D8-120; e=20 mm

In Fig.5.10, specimen D10-135 showed less moment capacity then the theoretical moment capacities. This might be due to the large tie spacing mentioned while discussing the load-strain curves in Section 5.2. In the moment-curvature diagram of specimen D10-135, a curve obtained from nagashima model for

unconfined case was also plotted. It seems that this curve also fitted the experimental ones satisfactorily.

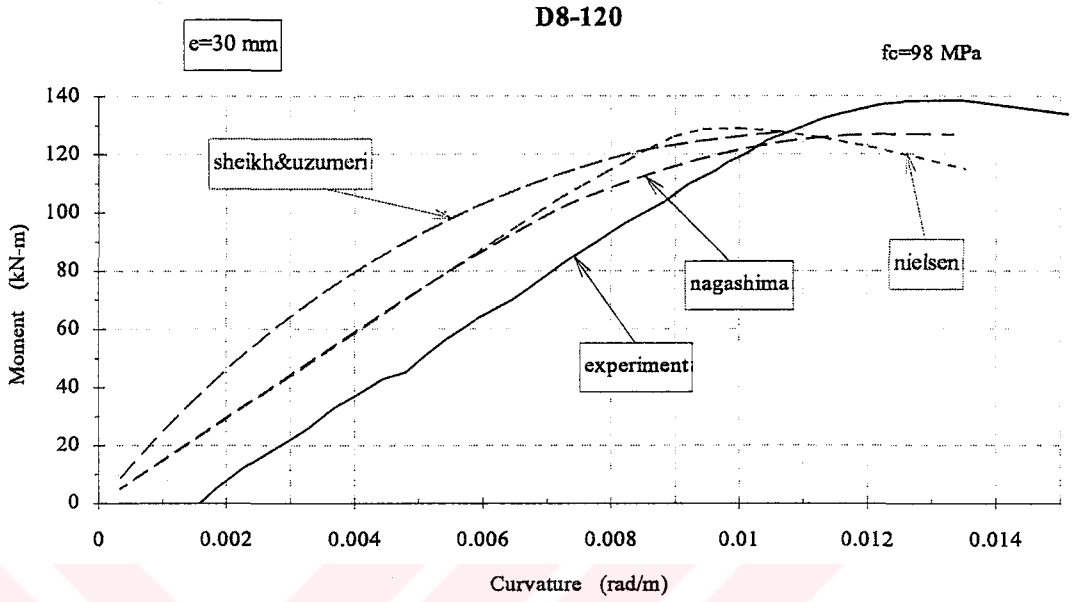

Figure 5.9 Comparison of moment-curvature curve of specimen D8-120; e=30 mm

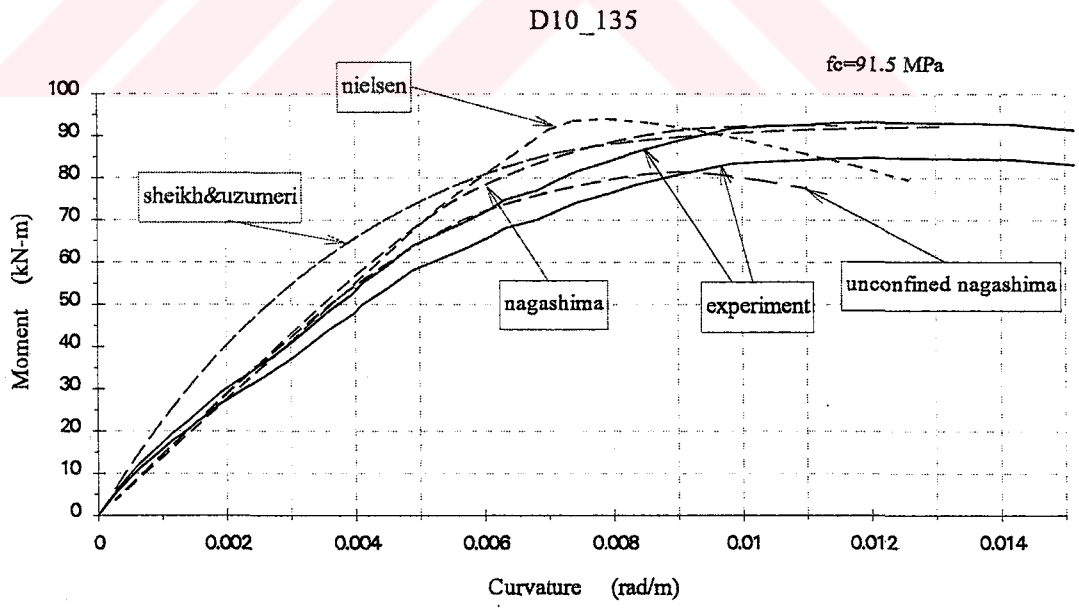

Figure 5.10 Comparison of moment-curvature curve of specimen D10-135

Fig.5.11 and Fig.5.12 show the moment-curvature curves of the specimens L8-75 and S8-75 respectively. In Fig.5.11, the analytical curve according to nagashima model showed quite acceptable fit to the experimental response. All the theoretical curves overestimated the specimen S8-75 in Fig.5.12. This difference may be due to the reasons explained at the beginning of this section. The expected behavior should have been at least that of the specimen L8-75. Neverthless, the variation between theoretical and experimental curve were not significant.

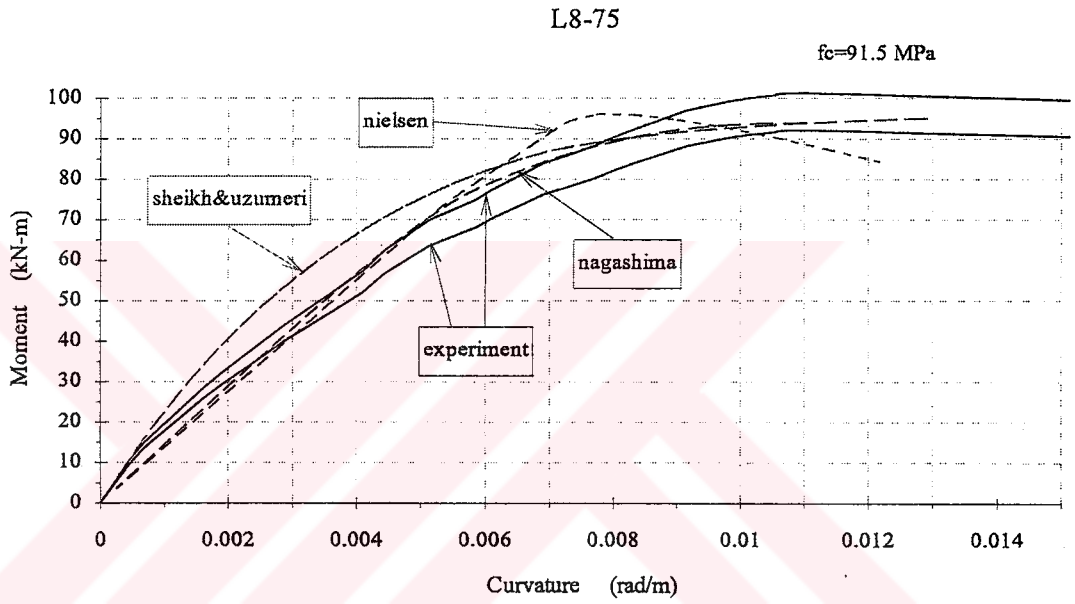

Figure 5.11 Comparison of moment-curvature curve of specimen L8-75

Specimen D8-75 (Fig.5.13) was loaded three times. Only the first and the last loadings are shown on the diagram. At the second loading of the specimen, load cell gave unreasonable readings. The analytical curve obtained from nagashima model predicted also in this test both the initial ascending portion and the moment carrying capacity quite satisfactoriliy.

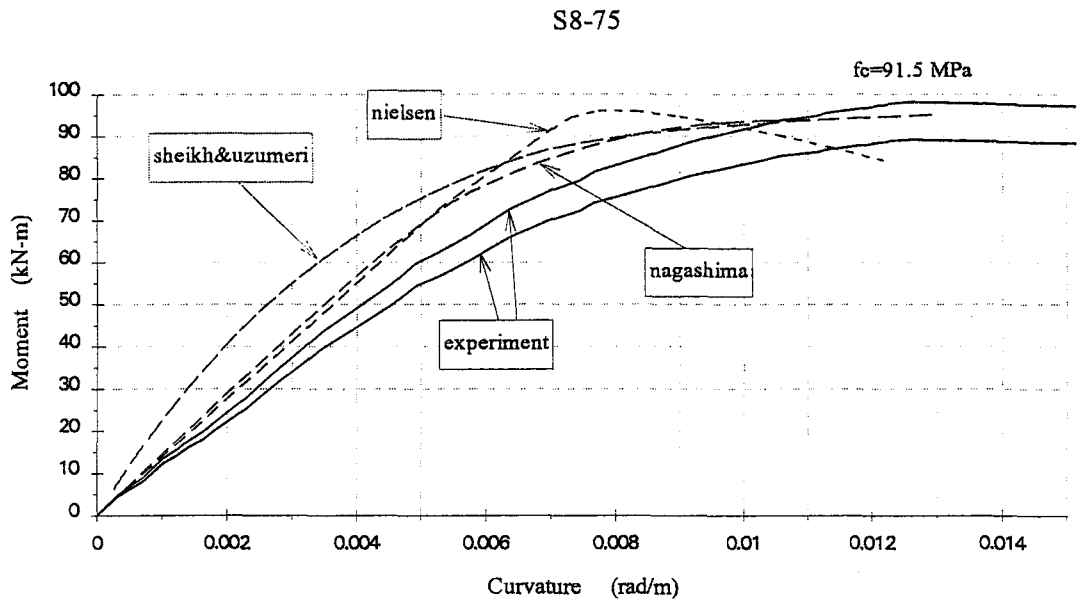

Figure 5.12 Comparison of moment-curvature curve of specimen S8-75

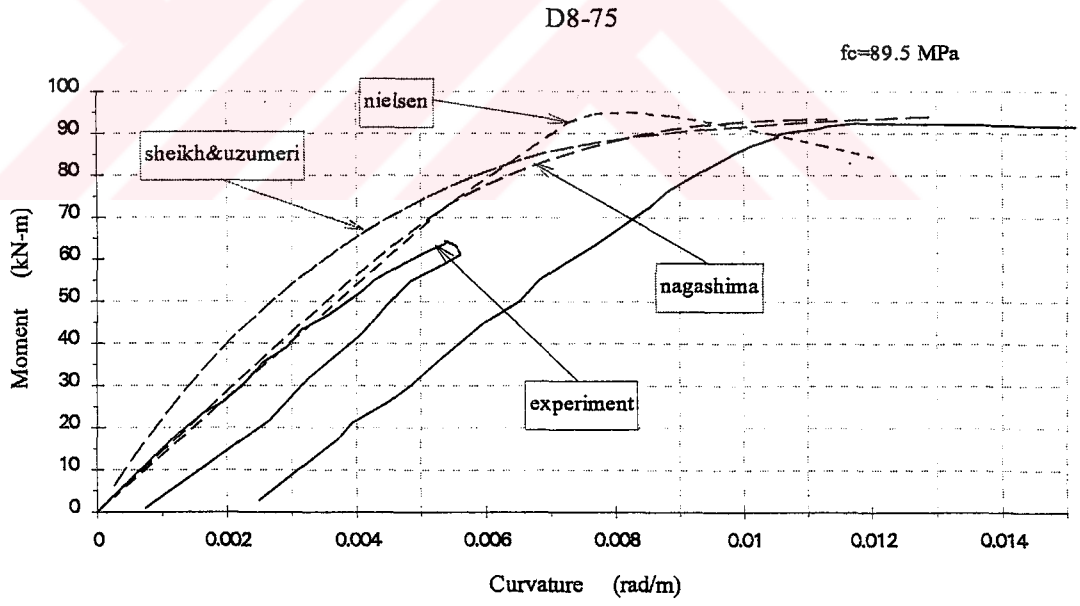

Figure 5.13 Comparison of moment-curvature curve of specimen D8-75

5.4 Comparison of the experimental data with the interaction diagrams

In this section, the moment and the normal force values (M,N) at the failure of specimens were marked on the analytically obtained interaction diagrams. Analytical curves were calculated from the three selected models. These models are described in Appendix A. For evaluating the analytical models a computer programme was developed. The procedure of the programme was as follows:

1. select a neutral axis depth, c
2. calculate the M-N values
3. increase the value of c and go to step 2
4. repeat this steps until a selected maximum neutral axis c, that could draw a complete interaction diagram

The interaction diagrams obtained by the above procedure are presented in Fig.5.14 to Fig.5.19. Both the experimental first order moments and the experimental total moments including the second order effects were marked on the diagram. The total moments were obtained by increasing the first order moments 10%. All analytical models used in this study predicted the experimental M-N pairs at failure of specimens satisfactorily. In all diagrams Nagashima curve constitute a lower bound on the compression failure portion of the interaction diagram (over the balanced case). At the tension failure zone all the three analytical curves were almost same. Therefore, the diagram according to Nagashima model is the conservative one among the three models used in this study.

The interaction diagram of the reference specimen is shown in Fig.5.14. The experimental M-N pairs corresponding to the failure of reference specimen fall quite out of the interaction diagrams. Therefore, the curves remained on the safe side according to the experimental point. The agreement between the analytical interaction curves and experimental ultimate points were quite satisfactorily.

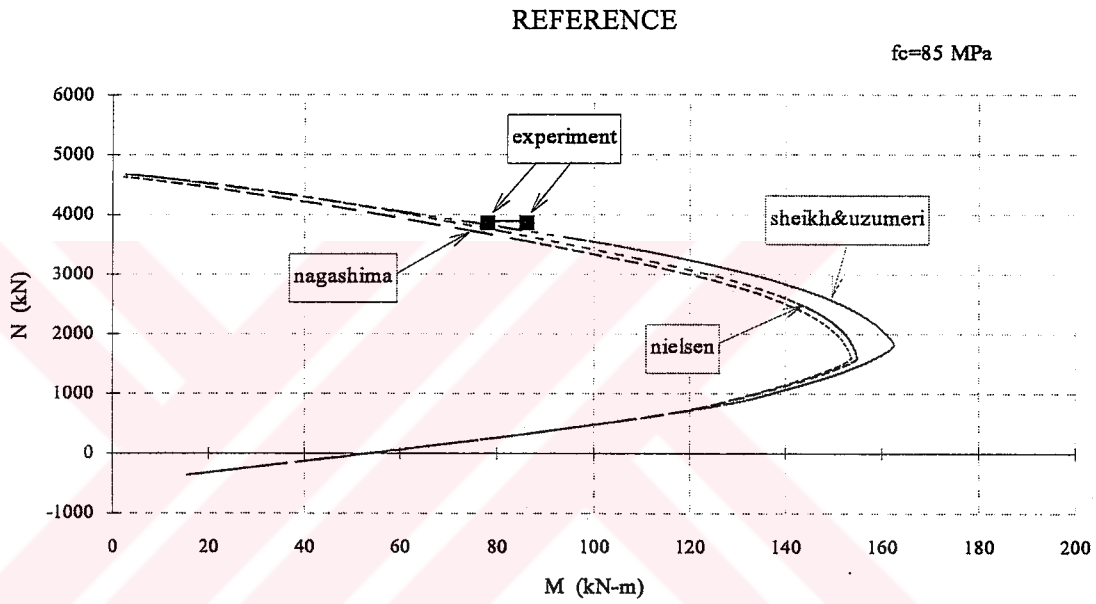

Figure 5.14 Interaction diagrams for specimen Reference

The experimental M-N pairs of specimen D8-120 (Fig.5.15) fell outside of the curves. Therefore the interaction curves obtained from the analytical models remained on the safe side. This diagram showed the biggest difference between the experimental and analytical moments. The variation was about 18 %.

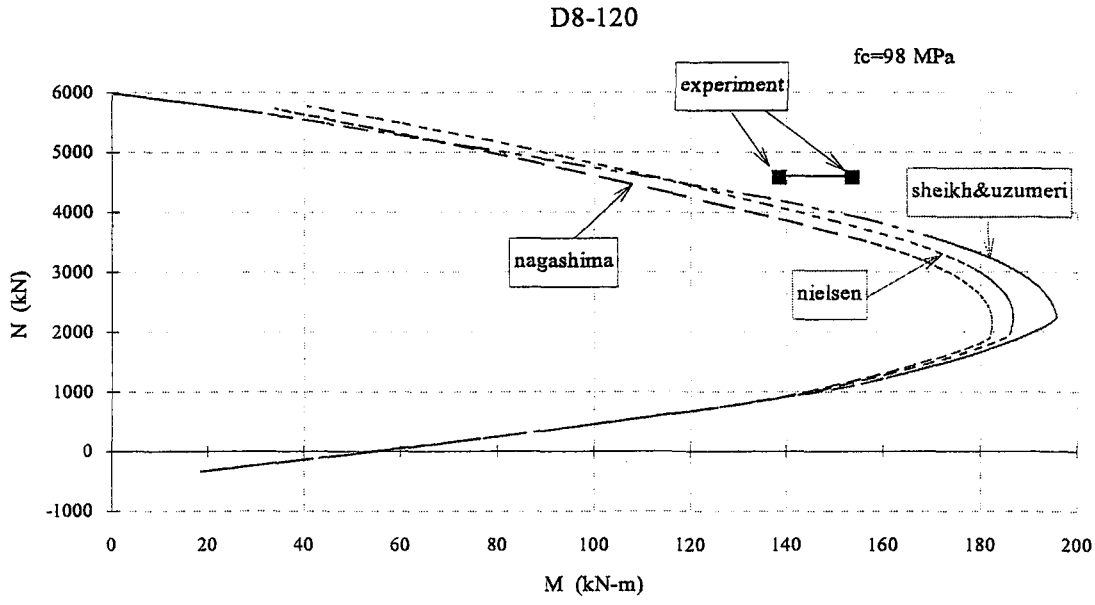

Figure 5.15 Interaction diagrams for specimen D8-120

In Fig.5.16, the (M,N) pair corresponding to the failure of specimen D10-135 fell inside the interaction diagrams, implying that all failure envelopes were unsafe. It seemed that the reason was the tie spacing as discussed in the load-strain and moment-curvature analysis (Sec.5.2 and Sec.5.3). Although the number of experiments were not sufficent to reach a general conclusion, it seems that if the tie spacing exceeds a maximum value, the expected confinement effect will not be achieved despite the fact that the diameter and yield strength of the lateral bars are increased according to the analytical calculation.

Fig.5.17 and Fig.5.18 shows the interaction diagrams of specimen L8-75 and S8-75 respectively. The agreement between the interaction diagrams obtained from

the analytical models and the M-N pair corresponding to the failure of specimen was quite satisfactorily.

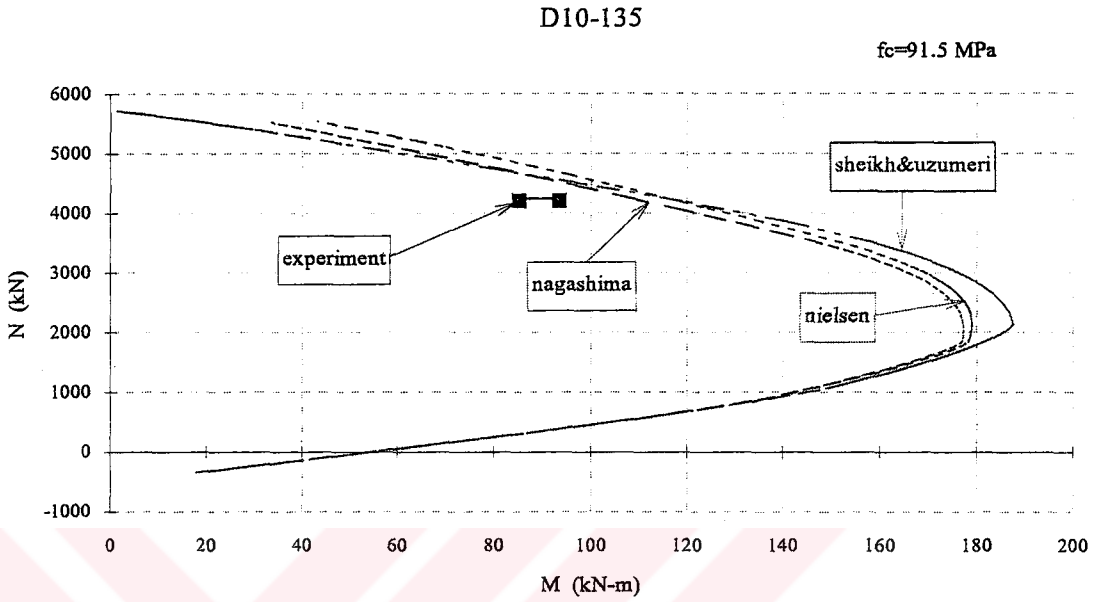

Figure 5.16 Interaction diagrams for specimen D10-135

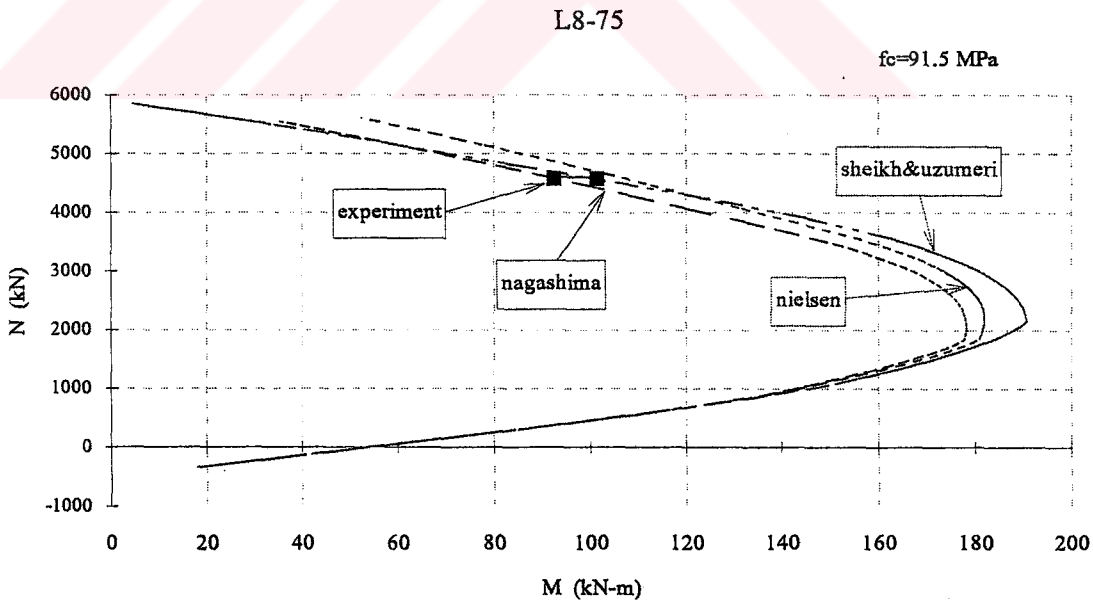

Figure 5.17 Interaction diagrams for specimen L8-75

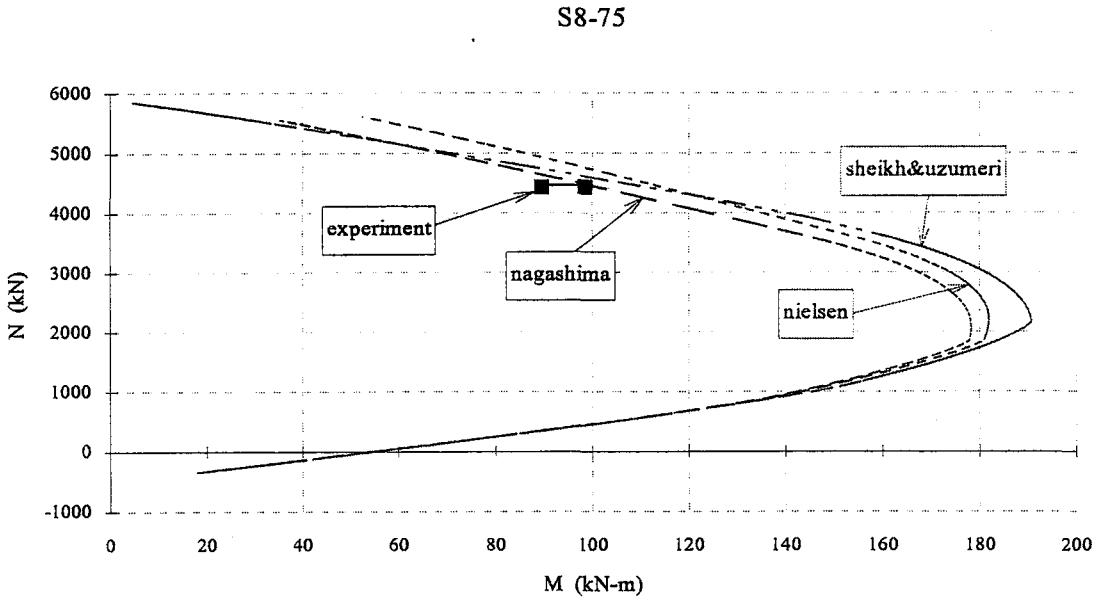

Figure 5.18 Interaction diagrams for specimen S8-75

All the three analytical interaction diagrams predicted in Fig.5.19 the experimental ultimate response satisfactorily.

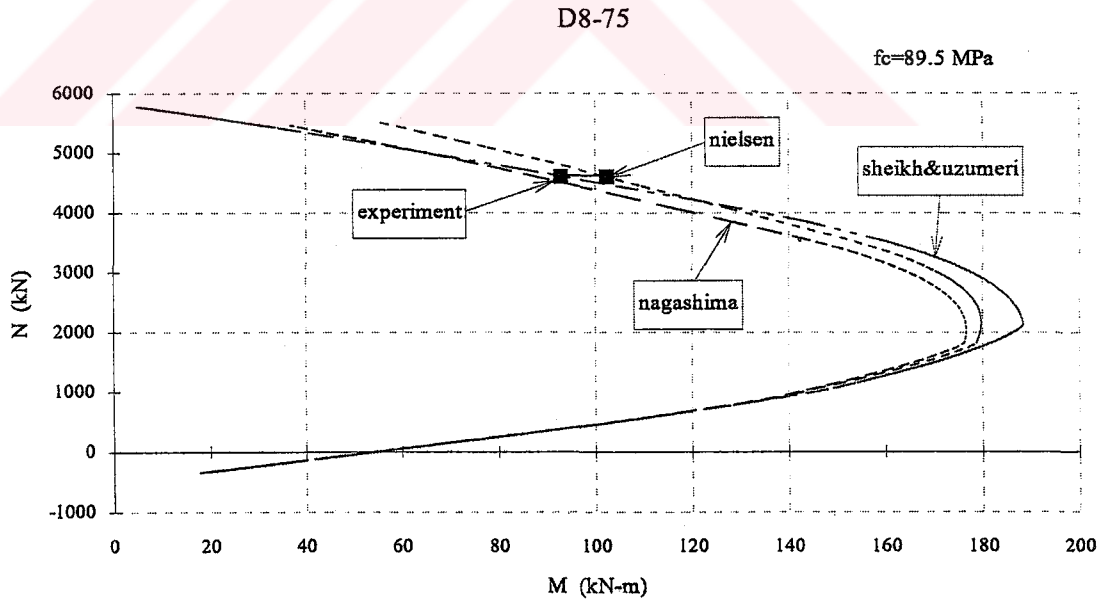

Figure 5.19 Interaction diagrams for specimen D8-75

5.5 Examination of the Poisson's Ratio

In this section, Poisson's ratio of the specimens are examined. Poisson's ratio is defined as the ratio of the transverse strain to the longitudinal strain. The Poisson's ratio changes significantly with the load level as the internal microcracks increase. At stress levels of σ_c/f_c=0.3-0.7 the Poisson's ratio is approximately 0.15-0.25 for NSC. In the CEB Recommendations and TS-500 it is specified as 0.20 approximately [3,40]. Experimental data on Poisson's ratio for high-strength concrete are limited. However, based on the available information, Poisson's ratio for HSC in the elastic range seems to be comparable to the expected range of values for lower strength concretes, approximately 0.18-0.24 depending on the stress level. In the inelastic range, the relative increase in the lateral strains is lower for HSC due to less micro cracking.

Poisson's ratio of the specimens are shown in Fig.5.20 to Fig.5.25. For specimen D8-120 the first loading was considered, in which the column was loaded concentrically (Fig.5.21). The first loading was also used by specimen D8-75 (Fig.5.25). Poisson's ratio was calculated at each load level by dividing the average lateral front strain to the average longitudinal front strain. Y axis was given as σ_c/f_c ratio. To find the concrete stress, first the force carried by steel was subtracted from the total force and then divided by the cross-sectional area. This concrete stress was normalized with respect to the concrete strength found from the concrete cylinder test. The Poisson's ratio points marked on the diagram was substituted with a single line to examine the trend of the Poisson's ratio variation with the increasing stress level. At low stress levels, the data points were not plotted, since the scatter was very high due to numerical errors.

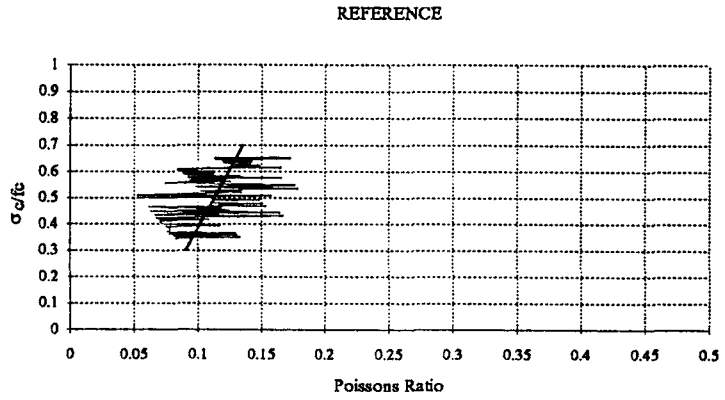

Figure 5.20 Poisson's ratio for specimen Reference

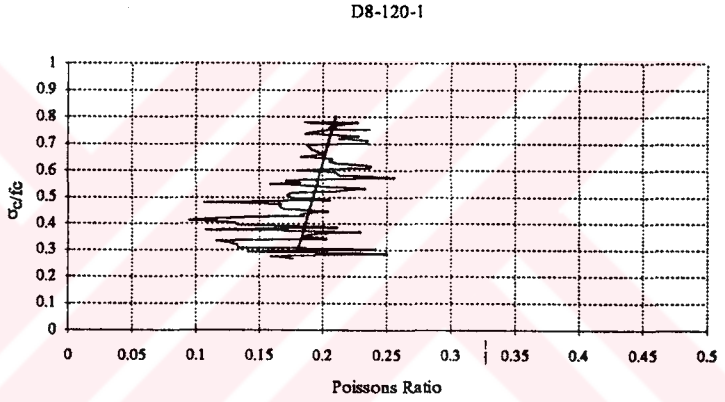

Figure 5.21 Poisson's ratio for specimen D8-120

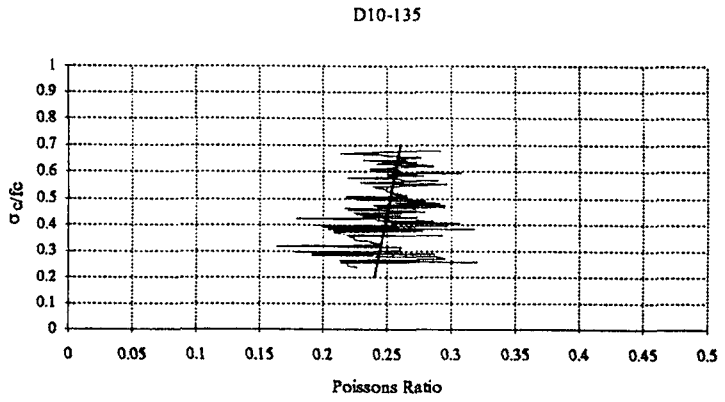

Figure 5.22 Poisson's ratio for specimen D10-135

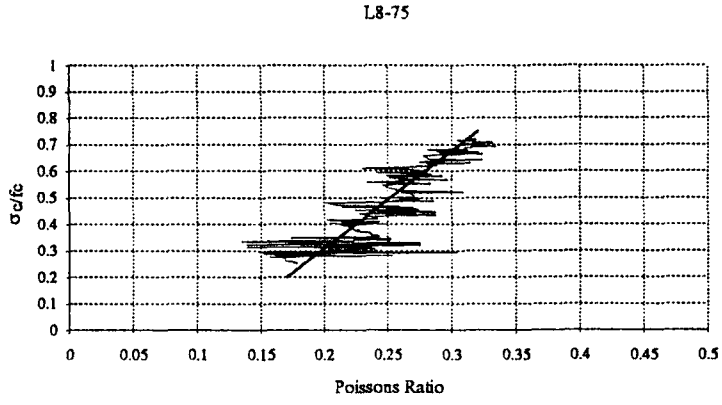

Figure 5.23 Poisson's ratio for specimen L8-75

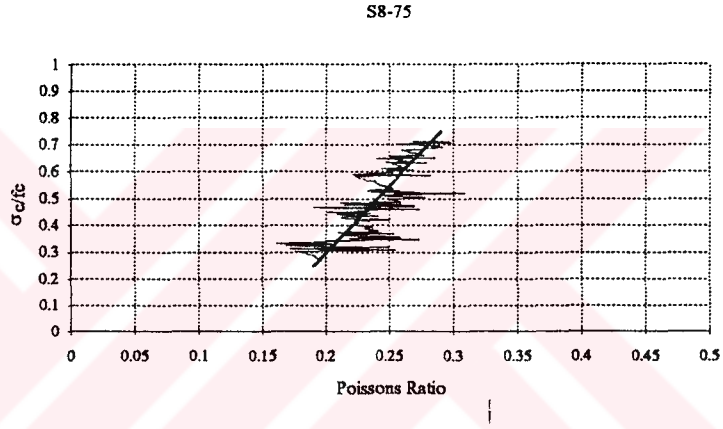

Figure 5.24 Poisson's ratio for specimen S8-75

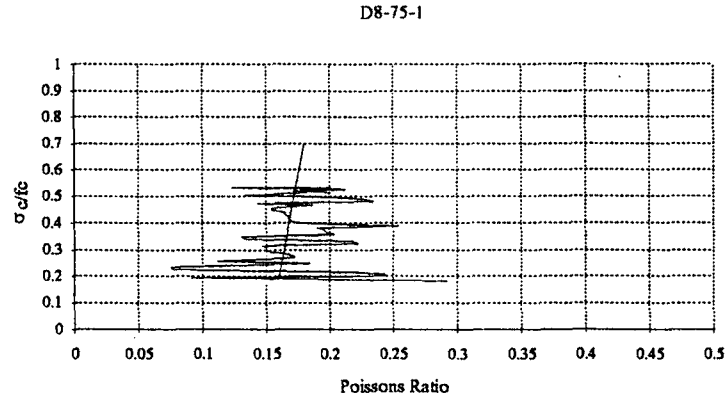

Figure 5.25 Poisson's ratio for specimen D8-75

The Poisson's ratio was read at the load levels of the 0.3 and 0.7 times of the maximum load. These values were given in Table 5.1. The average Poisson's ratio of the specimens varied between 0.18 and 0.23. Agreement between these values and the Poisson's ratio on HSC in literature were quite satisfactorily.

Table 5.1 The Poisson's ratio of the specimens

Specimen	**Poisson's ratio μ**	
	σ_c/f_c=0.3	σ_c/f_c=0.7
Reference	0.090	0.125
D8-120	0.180	0.205
D10-135	0.240	0.260
L8-75	0.200	0.305
S8-75	0.200	0.280
D8-75	0.160	0.180
Average	0.178	0.226

5.6 Strength and ductility comparisons

Lateral confinement of concrete columns creates a triaxial state of compression and therefore increases their strength and ductulity. In Table 5.2, strength gain of concrete of the specimens were compared. To calculate the force carried by steel, first steel strains were calculated by means of front and back strain

readings taken during the experiments. Force carried by concrete , N_{oc}, was calculated by subtracting the steel force, N_{os}, from the total force, N_{test}. To calculate average compression stress imposed on the section the concrete forces were divided by concrete strength, f_c,and the cross-sectional area, A_c. The average concrete stress was normalized with respect to the value of reference specimen so that they could be compared between each other. These calculations were tabulated in Table 5.2.

Table 5.2 Comparison of the strength gain of the concrete

	f_c (MPa)	f_y (MPa)	ρ_s (%)	$\rho_s f_y/f_c$ (%)	N_{test} (kN)	$N_{o,s}$ (kN)	$N_{o,c}$ (kN)	$\frac{N_{o,c}}{f_c A_c}$	Normalized wrt Ref.
Reference	85	323	--	--	3899	371	3528	0.664	1.000
D8-120	98	323	1.29	4.21	4617	398	4219	0.689	1.038
D10-135	91.5	375	1.77	7.27	4240	349	3891	0.680	1.025
L8-75	91.5	323	1.81	6.39	4602	356	4246	0.742	1.118
S8-75	91.5	323	1.81	6.39	4462	349	4113	0.719	1.083
D8-75	89.5	323	2.06	7.44	4619	351	4268	0.763	1.149

The confining cross-ties with 90° bend at one end in specimen L8-75 was tought to be less effective than the one with 135° bend at both ends provided in specimen S8-75. Nevertheless, the analysis in Table 5.2 proved that both type of cross-ties showed same efficiency. Canadian Standards Association, CSA A23.3-94 [42], stated: "cross ties shall have a standard hook with a bend of at least 135° at one end and a standard hook with a bend not less than 90° at the other end". This type of

cross-tie is preferable because it eases the construction and increases the construction speed.

Earlier discussions on load-strain diagrams, moment-curvature diagrams and interaction diagrams showed that specimen D10-135 did not demonstrate the expected behavior obtained from the analytical models. Specimen D10-135 and D8-75 had almost equal mechanical ratio. But according to Table 5.2, specimen D10-135 had only a strength enhancement of 2.5%, whereas specimen D8-75 had a strength enhancement of 15%. The reason for this might be the large tie spacing. Specimen D10-135 had a tie spacing of 135 mm. Minimum requirements for tie spacing found in the literature were listed below:

- Paulay and Priestley [39] proposed that the tie spacing should not exceed six times the diameter of the longitudinal bar to be restrained to avoid buckling of longitudinal reinforcement under compression load. According to this limitation maximum tie spacing in this test should be 84 mm.
- Turkish Building Code, TS500 [40], stated that tie spacing should be less or equal than 12 diameter of longitudinal reinforcement and 200 mm. This gave a maximum tie spacing of 168 mm for this study.
- Canadian Standards Association, CSA A23.3-94 [42], determined that the tie spacing shall not exceed the smallest of 16 times the diameter of the smallest longitudinal bars or 48 tie diameters or the least dimension of the compression member. The Code stated also that for specified concrete compressive strengths in excess of 50 MPa, the tie spacing determined above shall be multiplied by 0.75. According to these statements the maximum tie spacing should be 168 mm.

- American Concrete Institute, ACI 318.89 (revised 1992) [43], stated that the tie spacing shall not exceed the smallest of 16 times the diameter of the smallest longitudinal bars or 48 tie diameters or the least dimension of the compression member. According to these statements the maximum tie spacing should be 224 mm.

According to the Codes the maximum tie spacing should be 168 mm. But even a tie spacing of 135 mm in specimen D10-135 was not satisfactory. Therefore, a limitation should be put for maximum tie spacing for HSC. Although the number of experiments were not sufficient to reach a general conclusion, it seemed that the limitation of the Turkish Building Code, TS500, should be multiplied by 0.75 if concrete compressive strength exceed 50 MPa. So, this suggestion states that tie spacing should be less than or equal to 9 diameter of longitudinal reinforcement and 150 mm. This gives a tie spacing of 126 mm. Specimen D10-135 did not assure this statement. To support this proposal additional experiments should be performed.

In Table 5.3, the front strains at peak load were compared. In some cases, it was not easy to determine the peak strain since some columns were loaded successively. The strains were normalized with respect to the reference specimen according to the strength of concrete.

According to Table 5.3, reference specimen showed the minimum front strain at peak load. There was an improvement with the increasing confinement. Specimen D8-120 and D10-135 that had a mechanical ratio of 4-6% showed the smallest shift in ε_0. Specimen L8-75, S8-75 and D8-75 that had a mechanical ratio of about 7% showed the biggest shift in ε_0. But these strain enhancements were

parallel to the strength enhancement of the concrete. There was no change at the slope of descending part of the load-strain curves or there was no deformation ability at the peak stress. Therefore, no ductility improvement was observed during the tests.

Table 5.3 Comparison of the strain values corresponding to peak stresses

	f_c (MPa)	Strain ε_m	Normalized wrt. Ref.
Reference	85	0.0022	0.0022
D8-120	98	0.0032	0.0028
D10-135	91.5	0.0030	0.0028
L8-75	91.5	0.0031	0.0029
S8-75	91.5	0.0034	0.0032
D8-75	89.5	0.0032	0.0030

Specimen D8-75 showed a strength gain of about 15%; but no ductility enhancement was observed. This specimen had a mechanical ratio of 7.44% which was the maximum ratio among the specimens tested in this study. According to the literature survey the ductility limit migth be determined as follows:

- Nagashima et. al. [21] concluded that the capacity of lateral reinforcement normalized by strength of plain concrete ($A_s/(b*s)*f_{yh}/f_c''$) should be higher than 0.18 to prevent a sudden failure after that the maximum strength is reached. For

specimen D8-75 these values were: A_s=171.6 mm^2, b=222 mm, s=75 mm, f_{yh}=323 MPa, f_c"=0.85*89.5 MPa. The calculated value was 0.044. For this case the lateral reinforcement was 25% of the required value.

- Nishiyama et. al. [23] proposed that for 110 MPa concrete strength and 800 MPa yield strength of confining reinforcement the volumetric ratio should be more than 4% to prevent HSC prisms from brittle axial compression failure. This gave a mechanical ratio of 20%. For specimen D8-75 this ratio was equal to 7.44, which means the ratio used was about 25% of the required one.
- Saatcioglu and Razvi [28] concluded that the columns with a mechanical ratio, $\rho_s f_{yt}/f_c'$, of 14% and 22% produced favourable deformation characteristics for columns with 12-bar and 8-bar arrangements, respectively. For this case the supplied reinforcement in specimen D8-75 was about 33% of the one proposed by Saatcioglu.

According to these limitations the confining reinforcement in D8-75 was not sufficient for a ductile behavior. Increasing the mechanical ratio by decreasing the tie spacing would result in unrealistically small tie spacing. Therefore, for HSC, columns High Strength Steel should be used. For example, for specimen D8-75, if the tie spacing was decreased to 60 mm and if the yield strength of lateral reinforcement was increased to 800 MPa, the mechanical ratio increases from 7.44 to 23, which might show ductile behavior. New experiments should be carried out on HSC columns with high strength steel.

There were some studies on the extension length of the hooks. For instance, Itakura and Yagenji [20] concluded on uniaxially loaded HSC column experiments that tie bars having 135° hooks with six-diameter extension length

anchored in the core concrete were not effective compared to that with ten-diameter extension length. On the other hand, Ozden [32] used in his experiments 15 times tie bar diameter for extension length of 135° hooks to avoid any possible slippage failure of the lateral tie hooks during the test. He observed that all the specimen failures were accompanied by a snapping failure of the lateral tie and no tie-slippage failure was observed. The Turkish Building Code, TS500, stated that the extension length of the hooks should not be less than 4 times the diameter of the tie or 50 mm. The extension lengths of the hooks in this study were determined according to the Turkish Building Code, TS 500. Both for 8 mm and 10 mm ties, the extension length was chosen as 50 mm. No problem was observed due to the extension length of the hooks. In specimen L8-75, only one hook opened at failure on the back face of the column as concrete pass from compression to tension.

CHAPTER VI

SUMMARY AND CONCLUSION

6.1 Summary

In this experimental study six high strength concrete columns were tested under eccentric loading. All the specimens were 250 mm square in cross-section and 1500 mm in height. Eight longitudinal ∅14 mm bars were placed uniformly over the perimeter of the cross-section. The eccentricity was applied as 20 mm for all columns except for Specimen D8-120 since the concrete strength of this column was very high. The head of the specimen D8-120 failed prematurely at the third loading. The column was repaired and the head of the column was moulded again. Because of the time delay caused by these complications, concrete gained additional strength. For this reason, 30 mm eccentricity had to be used to test the specimen D8-120. The test variables in this experimental study are the tie spacing, mechanical ratio, the amount of lateral steel and cross tie efficiency.

Specimens were loaded to fail under monotonically increasing eccentric compression. For each specimen, longitudinal and transverse deformations along with the load readings are taken.

The strength and ductility characteristics of the columns at peak were examined. Agreement between the selected analytical models and the experimental response were studied. According to these analysis the effects of the test variables were studied.

6.2 Conclusions

The following conclusions were drawn from the experimental study of a limited scope, since the experiment was load controlled :

1. HSC columns showed extremely brittle behavior unless confined by transverse reinforcement.

2. Cross-ties with 90° hook at one end and 135° at the other end was almost as effective as the one with 135° hooks at both ends.

3. A mechanical ratio ($\rho_s * f_{yt}/f_c$) of 7% was not enough to achieve any ductility gain. It only prevented the explosive type of failure of the concrete column. This column showed a strength enhancement of approximately 15% compared with the unconfined reference specimen. No improvement was observed at the post peak region.

4. Minimum requirements in TS500 provision for ties was not sufficient for HSC.

5. Specimen D10-135, that satisfied the minimum requirements of the tie spacing in TS500 provision, did not show the expected response obtained from the theoretical models.

6. The statement in TS500 (12.3.3) might be revised as follows: "tie spacing should be less or equal than 12 diameter of longitudinal reinforcement and 200 mm. For specified concrete compressive strengths in excess of 50 MPa, the tie spacing determined above shall be multiplied by 0.75."

7. Among the three models used in the analytical study, the agreement of the Nagashima concrete model [21] with the experimental observations was satisfactory.

8. No tie-slippage was observed at the hooks of the lateral ties during the tests. Only a hook in specimen L8-75 opened at failure. This specimen showed the behavior predicted by the theoretical models.

9. The mechanical ratio was a very important variable. One way of increasing this ratio was increasing the yield strength of the lateral reinforcement, that could keep the mechanical ratio as high as required with a practical tie spacing. Therefore, with high strength concrete, high strength steel should be used.

6.3 Recommendations for future researches

HSC is a relatively new material. There are research needs in many areas to insure the proper application of this material. According to our experimental study following recommendations could be made for the future researches:

1. Experimental study should be performed on high strength concrete columns confined with high strength steel.

2. Columns should be tested with a mechanical ratio greater than 7%. According to other studies this ratio should be between 17% and 29%.

3 This type of experiment should be repeated with lower axial force and higher moment, that takes the failure from compression case to the balanced case.

4 The tie spacing should be studied as a main variable to determine a limitation for the maximum tie spacing of the column.

5. The extension length of the tie hooks might be experimentally analysed to determine an effective length for HSC columns.

REFERENCES

[1] Walraven, J., "High Strength Concrete: A Material for the Future?," Utilization of High Strength Concrete Proceedings, Symposium in Lillehammer, Norway, June 20-23, 1993, pp. 17-27

[2] _____, "Design Aspects of High Strength Concrete," FIB/CEB Bulletin d'Information, No:193, Decembre 1989

[3] _____, "High Strength Concrete, State of the Art Report, " FIB/CEB Bulletin d'Information, No:197, August 1990

[4] _____, "State-of-the-Art Report on High Strength Concrete," ACI Journal, Committee Report, Report no. ACI 363R-84, July-August 1984

[5] Carrasquillo, P.M., Carrasquillo, R.L., "Evaluation of the Use of Current Concrete Practice in the Production of High-Strength Concrete," ACI Materials Journal, Technical Paper, January-February 1988, pp. 49-54

[6] _____, "Research Needs for High Strength Concrete," ACI Materials Journal, Committee Report, Report no. ACI 363,1R-87, Nov.-Dec. 1987, pp.559-561

[7] Uzumeri, S.M., Ozden, S., "Yüksek Dayanımlı Betonun İnşaatta Kullanımı Konusunda Standartlar ve Yönetmeliklerdeki Gelişmeler," 2. Ulusal Beton Kongresi, Yüksek Dayanımlı Beton, May 1991, pp.159-178

[8] Cusson, D., Paultre, P, "High-Strength Concrete Columns Confined by Rectangular Ties," ASCE Journal of Structural Engineering, Vol.120, No.3, 1994, pp.783-804

[9] Burdette, E.G., Hilsdorf, H.K., "Behavior of Laterally Reinforced Concrete Columns," Journal of the Structural Division, Proceedings of the American Society of Civil Engineers, Vol.97, No.ST2, February 1971, pp.587-602

[10] Sheikh, S.A., Uzumeri, S.M., "Strength and Ductility of Tied Concrete Columns," Journal of the Structural Division, Proceedings of the American Society of Civil Engineers, Vol.106, No.ST5, May 1980, pp.1079-1101

[11] Park, R., Priestley, M.J.N., Gill, W.D., "Ductility of Square-Confined Concrete Columns," Journal of the Structural Division, Proceedings of the American Society of Civil Engineers, Vol.108, No.ST4, April 1982, pp.929-950

[12] Sheikh, S.A., "A Comparative Study of Confinement Models," ACI Journal, July-August 1982, pp.296-306

[13] Sheikh, S.A., Uzumeri, S.M., "Analytical Model for Concrete Confinement in Tied Columns," Journal of the Structural Division, Proceedings of the American Society of Civil Engineers, Vol.108, No.ST12, December 1982, pp.2703-2722

[14] Kent, D.C., Park, R., "Flexural Members with Confined Concrete," Journal of the Structural Division, Proceedings of the American Society of Civil Engineers, Vol.97, No.ST7, July 1971, pp.1969-1990

[15] Fafitis, A., Shah, S.P., "Lateral Reinforcement for High-Strength Concrete Columns," High-Strength Concrete, SP-87, ACI, 1985, pp.213-231

[16] Yong, Y.K., Nour, M.G., Nawy, E.G., "Behavior of Laterally Confined High-Strength Concrete under Axial Loads," Journal of Structural Engineering, ASCE, Vol.114, No.2, February 1988, pp.332-351

[17] Saatcioglu, M., Razvi, S.R., "Strength and Ductility of Confined Concrete," Journal of Structural Engineering, ASCE, Vol.118, No.6, June 1992, pp.1590-1607

[18] Galeota, D., Giammatteo, M.M., Marino, R., "Strength and Ductility of Confined High Strength Concrete," Earthquake Engineering, Tenth World Conference, Balkema, Rotterdam, 1992, pp.2609-2613

[19] Hatanaka, S., Tanigawa, Y., "Lateral Pressure Requirement for Compressive Concrete," Earthquake Engineering, Tenth World Conference, Balkema, Rotterdam, 1992, pp.2603-2608

[20] Itakura, Y., Yagenji, A., "Compressive Test on High-Strength R/C Columns and their Analysis based on Energy Concept," Earthquake Engineering, Tenth World Conference, Balkema, Rotterdam, 1992, pp.2599-2602

[21] Nagashima, T., Sugamo, S., Kimura, H., Ichikawa, A., "Monotonic Axial Compression Test on Ultra-High-Strength Concrete Tied Columns," Earthquake Engineering, Tenth World Conference, Balkema, Rotterdam, 1992, pp.2983-2989

[22] Collins, M.P., Mitchell, D., MacGregor, J.G., "Structural Design Considerations for High-Strength Concrete," Concrete International, The Magazine of the American Concrete Institute, May 1993, Vol.15, No 5, pp.27-34

[23] Nishiyama, M., Fukushima, I., Watanabe, F., Muguruma, A., "Axial Loading Tests on High-Strength Concrete Prisms Confined by Ordinary and High-Strength Steel," Utilization of High Strength Concrete Proceeding, Symposium in Lillehammer, Norway, June 1993, pp.322-329

[24] Al-Hussaini, A., Regan, P.E., Xue, H.Y., Ramdane, K.E., "The Behaviour of HSC Columns under Axial Load," Utilization of High Strength Concrete Proceeding, Symposium in Lillehammer, Norway, June 1993, pp.83-90

[25] Azizinamini, A., Kuska, S.S.B., "Flexural Capacity and Ductility of High-Strength Concrete Columns ," Utilization of High Strength Concrete Proceeding, Symposium in Lillehammer, Norway, June 1993, pp.91-98

[26] Cusson, D., Paultre, P., "Experimental Study of High-Strength Concrete Columns Confined by Rectangular Ties," Utilization of High Strength Concrete Proceeding, Symposium in Lillehammer, Norway, June 1993, pp.136-145

[27] Muguruma, H., Nishiyama, M., Watanabe, F., "Stress-Strain Curve Model for Concrete with a Wide-Range of Compressive Strength," Utilization of High Strength Concrete Proceeding, Symposium in Lillehammer, Norway, June 1993, pp.314-321

[28] Saatcioglu, M., Razvi, S.R., "Behavior of High-Strength Concrete Columns Cnfined with Rectilinear Ties," Proceedings of the 5th U.S. National Conference on Earthquake Engineering, Earthquake Engineering Research, 1994, pp.629-638

[29] Cusson, D., Paultre, P., "High-Strength Concrete Columns Confined by Rectangular Ties," Journal of Structural Engineering, ASCE, Vol.120, No.3, March 1994, pp.783-804

[30] Razvi, S.R., Saatcioglu, M., "Strength and Deformability of Confined High-Strength Concrete Columns," ACI Structural Journal, V.91, No.6, November-December 1994, pp.678-687

[31] Polat, M.B., "Behaviour of Normal and High Strength Concrete under axial Compression," M.A.Sc. Thesis, Department of Civil Engineering, University of Toronto, Toronto, Canada, 1992

[32] Ozden, S., "Behaviour of High-Strength Concrete under Strain Gradient," M.A.Sc. Thesis, Department of Civil Engineering, University of Toronto, Toronto, Canada, 1992

[33] Nielsen, K.H., "Ductility of Sections Designed in High Strength Concrete," Utilization of High Strength Concrete Proceeding, Symposium in Stavanger, Norway, June 1987, Tapir, pp.535-546

[34] Baalbaki, W., Aïtcin, P.C., Ballivy, G., "On Predicting Modulus of Elasticity in Hifg-Strength Concrete," ACI Materials Journal, Technical Paper, September-October 1992, V.89, No 5, pp. 517-520

[35] Ersoy, U., "Reinforced Concrete," Middle East Technical University, Ankara, 1991

[36] Ersoy, U., Wasti, S.T., "Introductory Mechanics of Deformable Bodies," Middle East Technical University, Ankara, 1992

[37] Ferguson, P.M., "Reinforced Concrete Fundementals," John Wiley&Sons, Inc., Newyork, Second Edition, 1965

[38] Radain, T.A., Samman, T.A., Wafa, F.F., "Mechanical Properties of High-Strength Concrete," Utilization of High Strength Concrete Proceeding, Symposium in Lillehammer, Norway, June 1993, pp.1209-1216

[39] Paulay, T., Priestley, M.J.N., "Seismic Design of Reinforced Concrete and Masonry Buildings," John Wiley&Sons, Inc., 1992

[40] _____, TS500, "Betonarme Yapıların Hesap ve Yapım Kuralları," "Building Code Requirements for Reinforced Concrete," Ankara, 1985

[41] Tumer, O., "Uniaxially Loaded High Strength Concrete Spiral Columns," M.A.Sc. Thesis, Department of Civil Engineering, Middle East Technical University, Ankara, 1995

[42] _____, "A23.3 Design of Concrete Structures," Canadian Standards Association, Rev.8.0, 1994

[43] _____, "Building Code Requirements for Reinforced Concrete (ACI 318M-89) and Commentary (ACI 318RM-89, metric version), American Concrete Institute, Detroit, 1990

[44] Soliman, M.T.M., Yu, C.W., "The Flexural Stress-Strain Relationship of Concrete Confined by Rectangular Transverse Reinforcement," Magazine of Concrete Research, Vol.19, No.61, Dec. 1967, pp. 223-238

[45] Roy, H.E.H., Sozen, M.A., "Ductility of Concrete," Proceedings of the International Symposium on Flexural Mechanics of Reinforced Concerete, ASCE-ACI, Miami, Nov. 1964, pp.213-224

[46] Bertero, V.V., Felippa, C., discussion of "Ductility of Concrete," by Roy, H.E.H., Sozen, M.A., Proceedings of the International Symposium on Flexural Mechanics of Reinforced Concerete, ASCE-ACI, Miami, Nov. 1964, pp.213-224

APPENDIX A

CONCRETE STRESS - STRAIN MODELS

A.1. General

In this chapter the stress-strain models for concrete used throughout this study is explained. Three models are studied: Nielsen, Sheikh&Uzumeri and Nagashima et. al. There are many other models that can be applied to the experimental work; but it is avoided to study numerous numbers of models. According to the other analytical studies, such as papers on HSC or other master thesis on HSC [31,32], these three models are worth to be selected. The other models, for instance Kent&Park and its modified versions, Bjerkeli et. al., Mander et. al., Muguruma et. al. or Thorenfeldt et. al., etc., could not fit the experimental curves in a satisfactory manner. The reason of the inefficiency of some curves comes from the fact that they are derived from the results of experimental works based on normal strength concrete. On the other hand, some other ones could not reflect the behavior of the columns adequately, despite the fact that they are derived for high strength concrete.

A.2. Nielsen

This curve is selected due to its simplicity. The Nielsen concrete stress-strain curve [33] is for plain HSC and has a triangular shape. In this study, it is used for confined concrete with a modification. The maximum stress and the strain at maximum stress are multiplied with a factor, Ks. This factor is the strength gain factor emerge from the confinement. In fact, the strength gain factor is firstly calculated in Sheikh&Uzumeri model and then adopted by Nielsen model. It shows the ratio of confined strength to unconfined strength of concrete. Fig.5.1 shows both the original Nielsen unconfined stress-strain curve and our modification for confined concrete.

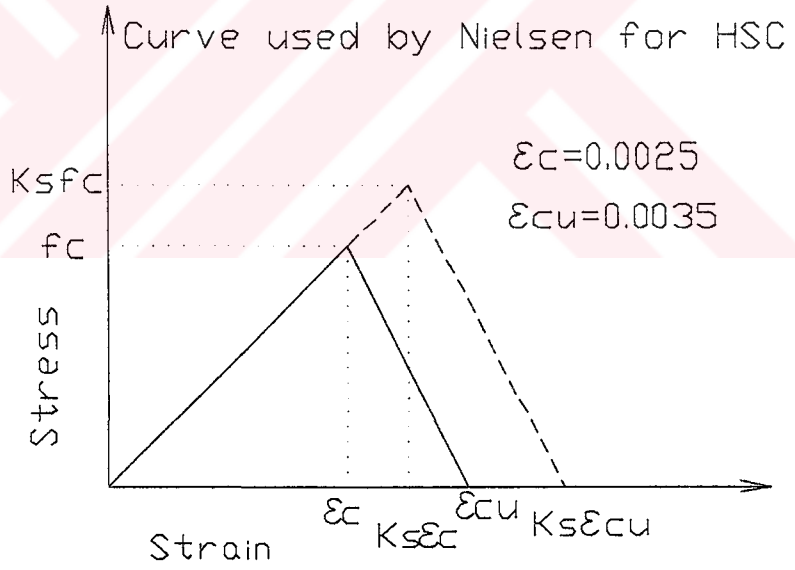

Figure A.1 Nielsen concrete stress-strain curve

A.3. Sheikh & Uzumeri

The Sheikh & Uzumeri model was developed primarily from the results of the 24 columns tested under concentric axial load at the University of Toronto [13]. The test variables are reported as: volumetric ratio and spacing of the tie steel, characteristics of the steel, distribution of the longitudinal steel around the perimeter, and the resulting tie configuration. The effectively confined area is defined as the area between the center lines of the outer perimeter hoop less the unconfined area in between the longitudinal steels. The model mainly assumes that in order for a longitudinal bar to be effective in confinement, it must be fully supported by a bend of a tie.

The curve consists of three parts. Part OA is a second degree parabola with point A at f_{cc}, ε_{s1}. Term f_{cc} represents the compressive strength of confined concrete in the specimen and is equal to $K_s f_{cp}$, in which f_{cp} = the compressive strength of concrete in plain specimen; K_s = the strength gain factor. The ε_{s1} and the ε_{s2} are the minimum and the maximum strain values respectively corresponding to the maximum stress. The ε_{s85} is the value of strain corresponding to 85% of the maximum stress on the unloading branch of the curve. Parts AB and BC of the curve are straight lines. Beyond point C, the curve can be expected to continue in the same straight line until the stress is dropped to about 30% of the maximum value (point D). Beyond point D, a horizontal line can be assumed to represent concrete behavior. Fig.5.2 shows Sheikh&Uzumeri confined stress-strain model in detail.

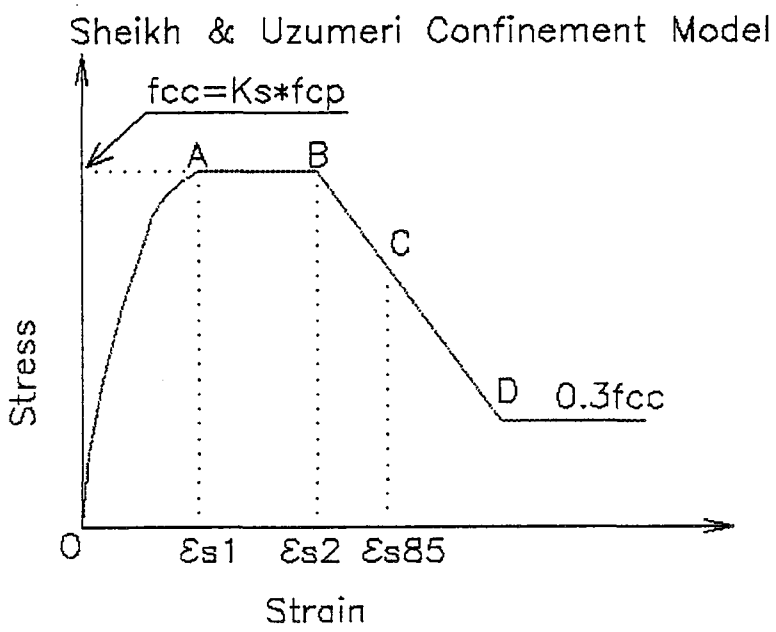

Figure A.2 Sheikh & Uzumeri confined stress-strain model

The parameters of the curve are calculated as follows:

$$K_s = 1.0 + \frac{B^2}{140 \cdot P_{occ}} \left[\left(1 - \frac{nC^2}{5.5 \cdot B^2} \right) \left(1 - \frac{s}{2 \cdot B} \right) \right] \sqrt{\rho_s \cdot f'_s}$$

Ks : The ratio of confined strength to unconfined strength of concrete; this equation is valid only for square sections with uniformly distributed longitudinal steel.

P_{occ} : unconfined strength of concrete core (kN)

$$P_{occ} = 0.85 \cdot \frac{f'_c}{1000} \cdot (A_{oc} - A_s)$$

$$A_{oc} = B \times H$$

A_{oc} : the core area enclosed by the center line of outer tie (mm^2)

A_s : the total area of the longitudinal steel

f_c' : concrete cylinder strength (MPa)

f_s' : the stress in the lateral steel at the time of maximum resistance of confined concrete (MPa)

B,H : the center-to-center distance of perimeter tie of rectangular core (mm)

n : the number of arcs

C : the center-to-center distance between longitudinal bars (mm)

s : tie spacing (mm)

ρ_s : the ratio of the volume of total lateral reinforcement to the volume of core

$$\varepsilon_{s1} = 80 \cdot K_s \cdot f_c' \times 10^{-6}$$

later modified as : $\varepsilon_{s1} = \varepsilon_0 \cdot K_s$ where $\varepsilon_0 = 0.0022$

ε_0 : strain corresponding to the maximum stress in plain concrete

$$\frac{\varepsilon_{s2}}{\varepsilon_0} = 1 + \frac{248}{C}\left[1 - 5.0\left(\frac{s}{B}\right)^2\right]\frac{\rho_s f_s'}{\sqrt{f_c'}}$$

$$\varepsilon_{s85} = \frac{0.15}{Z} + \varepsilon_{s2}$$

where $$Z = \frac{0.5}{\frac{3}{4}\rho_s\sqrt{\frac{B}{s}}}$$

A.4. Nagashima

The Nagashima model was developed from the results of twenty-six specimens of HSC and UHSC, which were reinforced laterally with high or ultra-high strength steel bars [21]. High strength longitudinal reinforcing bars were also provided. The proposed model satisfactorily predicted the experimental stress-strain curves for concrete strength up to 118 MPa.

$$f_c = \frac{f_{cc} \cdot x \cdot r}{r - 1 + x^r} \qquad \text{for} \; 0 < \varepsilon_c \le \varepsilon_{cm}$$

$$x = \frac{\varepsilon_c}{\varepsilon_{cm}}$$

$$r = \frac{E_c}{E_c - E_{sec}}$$

$$E_{sec} = \frac{f_{cc}}{\varepsilon_{cm}}$$

$$f_c = f_{cc} \cdot \left[1 - 0.5 \cdot \frac{\varepsilon_c - \varepsilon_{cm}}{\varepsilon_{50} - \varepsilon_{cm}}\right] \ge 0.3 \cdot f_{cc} \qquad \text{for} \; \varepsilon_{cm} < \varepsilon_c$$

f_c : longitudinal stress in concrete (kg/cm^2)

ε_c : longitudinal strain in concrete (kg/cm^2)

f_{cc} : maximum stress in confined concrete (kg/cm^2)

ε_{cm} : strain at maximum stress in confined concrete (kg/cm^2)

E_c : tangent modulus of elasticity of plain concrete (kg/cm^2)

ε_{50} : strain at 0.5 f_{cc}

$$f_{cc} - f_c'' = 31.4 \cdot \sqrt{\lambda^* \cdot \rho'_w \cdot f_{yh}}$$

f_c'' : the strength of unconfined concrete (kg/cm^2)

$$f_c'' = 0.85 \cdot f'_c$$

fc' : compressive strength of 100ϕx200 mm cylinder test

f_{yh} : yield strength of lateral reinforcement

λ^* : a simplified form of the reduction factor proposed by Sheikh & Uzumeri

$$\lambda^* = \left(1 - \frac{\sum C_i^2}{6 \cdot B^2}\right) \cdot \left(1 - \frac{s}{2 \cdot B}\right)^2$$

C_i : the center-to-center distance between longitudinal perimeter bars

B : the center-to-center distance of a perimeter tie around the square core

s : the tie spacing

ρ'_w : area ratio of lateral reinforcement

$$\rho'_w = \frac{A_s}{B \cdot s}$$

A_s : total area of lateral reinforcement

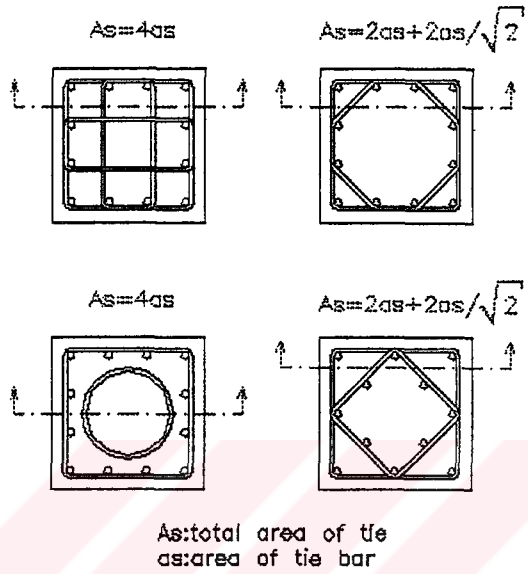

Figure A.3 Calculation of the total area of the lateral reinforcement

$$\frac{\varepsilon_{cm}}{\varepsilon_m} = 138 \cdot \left(\lambda^* \cdot \rho'_w \cdot \frac{f_{yh}}{f''_c} \right)^2 + 1$$

ε_m : the strain at the maximum stress of unconfined concrete

$$\varepsilon_m = \varepsilon_0$$

ε_0 : the strain at the maximum stress of 100ϕx200 mm cylinder test

Collins and Mitchell [22] suggested that

$$\varepsilon_m = \frac{f'_c}{E_c} \cdot \frac{n}{n-1}$$

where $$n = 0.8 + \frac{f'_c}{17} \qquad \text{(MPa)}$$

E_c is calculated from the equation of ACI 363 [4,34]:

$$E_c = 3320 \cdot \sqrt{f'_c} + 6900 \qquad \text{(MPa)}$$

ε_{50} is selected to determine the descending part of the stress-strain curve. ε_{85}.is assumed to be inconvenient for this case since the slope of the descending part is very sensitive for this strain ε_{85}. The following equation for ε_{50} is derived from a regression analysis:

$$\varepsilon_{50} = \varepsilon_m + 0.193 \cdot \left(\lambda^* \cdot \rho'_w \cdot \frac{f_{yh}}{f''_c} \right)$$

If there is no lateral steel in the specimen, then ε_{50} will be equal to ε_m. This will cause 'dividing by zero error' at the calculation of f_c in the region of $\varepsilon_{cm} < \varepsilon_c$. To prevent this error we assume that ε_{50} = 1.15 ε_m . In return with the specimen Reference ε_m =0.0028 and ε_{50} =0.00322, which is quite acceptable.